

## Review Article

Nur Aliaa Zulkefli, Rohani Mustapha\*, Suriani Mat Jusoh, Che Mohd Ruzaidi Ghazali, Mohamad Awang\*, Mohd Nor Faiz Norrrahim\*, and Rushdan Ahmad Ilyas

# Hybrid nanofiller reinforcement in thermoset and biothermoset applications: A review

<https://doi.org/10.1515/ntrev-2022-0499>

received March 25, 2022; accepted September 29, 2022

**Abstract:** Thermoset and biothermoset applications have been advancing tremendously in recent years due to their easy processing, versatility, and exceptional mechanical and thermal properties. Biothermoset is a type of thermoset that is produced using biological resources, either in portions by blending with the conventional resin, or completely. Various research has been employed to accommodate their high and rapidly growing demands and broaden their functions and implementation in numerous fields. One of these attempts is the reinforcement of nanofillers. Nanofillers such as nanoclay, graphene nanoplatelets, carbon nanotubes, nanodiamond, *etc.*, possess diverse and outstanding properties and are also easily accessible.

Recently, there has been a developing trend of hybridizing two or more types of nanofillers as a hybrid reinforcement system to address the limitations of single-filler reinforcement systems and to establish better-supporting properties of the nanocomposites. In this review, we discussed the use of hybrid nanofillers in different thermoset and biothermoset applications. Emphasis is given to the types of hybrids, their interactions with each other and the host polymer, and the effects of their contents and ratios. Limitations from the previous works are also discussed and the future undertaking of research on hybrid nanofillers is also proposed.

**Keywords:** thermoset, biothermoset, nanofiller, hybrid, electronic, thermal management, tribological

## List of abbreviations

|      |                                 |
|------|---------------------------------|
| AgNF | silver nanoflake                |
| AgNW | silver nanowire                 |
| AlN  | aluminum nitride                |
| BMI  | bismaleimide                    |
| BN   | boron nitride                   |
| CB   | carbon black                    |
| CD   | carbon dot                      |
| CFRP | carbon fiber-reinforced plastic |
| CNT  | carbon nanotube                 |
| COF  | coefficient of friction         |
| CS   | chitosan                        |
| EG   | expanded graphite               |
| EM   | electromagnetic                 |
| EP   | epoxy                           |
| ESOA | epoxidized soybean oil acrylate |
| FA   | furfurylamine                   |
| FrGO | fluorinated graphene oxide      |
| GNP  | graphene nanoplatelet           |
| GF   | gauge factor                    |
| GO   | graphene oxide                  |
| h-BN | hexagonal boron nitride         |
| HNT  | halloysite nanotube             |

\* **Corresponding author: Rohani Mustapha**, Faculty of Ocean Engineering Technology and Informatics, Universiti Malaysia Terengganu, Kuala Nerus 21030, Terengganu, Malaysia, e-mail: rohani.m@umt.edu.my

\* **Corresponding author: Mohamad Awang**, Faculty of Ocean Engineering Technology and Informatics, Universiti Malaysia Terengganu, Kuala Nerus 21030, Terengganu, Malaysia, e-mail: mohamada@umt.edu.my

\* **Corresponding author: Mohd Nor Faiz Norrrahim**, Research Centre for Chemical Defence, Universiti Pertahanan Nasional Malaysia (UPNM), Kuala Lumpur 57000, Malaysia, e-mail: faiz@upnm.edu.my

**Nur Aliaa Zulkefli**: Faculty of Ocean Engineering Technology and Informatics, Universiti Malaysia Terengganu, Kuala Nerus 21030, Terengganu, Malaysia, e-mail: nuraliaazulkefli@gmail.com

**Suriani Mat Jusoh**: Faculty of Ocean Engineering Technology and Informatics, Universiti Malaysia Terengganu, Kuala Nerus 21030, Terengganu, Malaysia, e-mail: surianimatjusoh@umt.edu.my

**Che Mohd Ruzaidi Ghazali**: Faculty of Ocean Engineering Technology and Informatics, Universiti Malaysia Terengganu, Kuala Nerus 21030, Terengganu, Malaysia, e-mail: ruzaidi@umt.edu.my

**Rushdan Ahmad Ilyas**: Department of Chemical Engineering, Faculty of Chemical and Energy Engineering, Universiti Teknologi Malaysia, Johor Bahru 81310, Malaysia; Institute of Tropical Forestry and Forest Products, Universiti Putra Malaysia, UPM Serdang, 43400, Selangor, Malaysia, e-mail: ahmadilyas@utm.my

|       |   |
|-------|---|
| HRR   | heat release rate   |
| MAM   | microwave absorbing material  |
| MMT   | montmorillonite   |
| MWCNT | multiwalled carbon nanotube   |
| NC    | nanoclay  |
| ND    | nanodiamond   |
| PANI  | polyaniline   |
| PAN   | poly(acrylonitrile)   |
| PBSF  | poly (butylene sebacate- <i>co</i> -butylene fumarate)  |
| PDA   | polydopamine  |
| PEI   | polyetherimide  |
| PEIS  | sulfonated polyetherimide   |
| PFB   | furfurylamine (FA)-functionalized dynamic covalently bismaleimide (BMI) cross-linked poly (butylene sebacate- <i>co</i> -butylene fumarate)           |
| PFBC  | furfurylamine (FA)-functionalized dynamic covalently bismaleimide (BMI) cross-linked poly (butylene sebacate- <i>co</i> -butylene fumarate) composite |
| PN    | polyaniline nanofiber   |
| POSS  | polyhedral oligomeric silsesquioxane  |
| PU    | polyurethane  |
| RGO   | reduced graphene oxide  |
| RL    | return loss   |
| RPUF  | rigid polyurethane foams  |
| SEM   | scanning electron microscope  |
| TA    | tetraaniline  |
| TEM   | transmission electron microscope  |
| THR   | total heat release  |
| TIM   | thermal interface material  |
| TSP   | total smoke production  |
| UPE   | unsaturated polyester   |

## 1 Introduction

In recent years, thermosetting polymeric materials have become one of the most vastly used high-performance engineering materials in various industries due to their excellent mechanical strength, electrical and thermal conductivity, fatigue and corrosion resistance, *etc.*, as well as their easy processing and broad structural versatility [1,2]. Their applications include automotive, aerospace, aeronautics, information technology, civil engineering, medical equipment, defense system, machinery, advanced sensing, electronic devices, *etc.* Thus, consistent with the rapid development of these materials and devices, vigorous research is conducted worldwide including a multitude of studies on

the effect of the inclusion of reinforcement additives into polymer composites including fibers [3–6], fillers [5–8], nanofillers [5,6,9–13], *etc.*

Additionally, the field of technology is also rapidly advancing. A multitude of innovative materials and devices can be generated by directly targeting the particular aspects or properties on the nanoscale level. These advancements comprise the fields of medicine [14–16], pharmaceutical [15,17], manufacturing [18], agriculture [19], and also polymer composites [20]. Polymer nanocomposite is a class of materials that contains two or more phases of different structures, and one of their dimensions is at the nanometer level. The nanocomposite is usually dispersed with organic/inorganic, or natural/synthetic nanofillers [21].

Nanofillers are particles with sizes ranging from 1–100 nm [22] with various types and morphology (Figure 1). Nanoclay (NC), graphene, carbon nanotube (CNT), boron nitride (BN), silicon dioxide (SiO<sub>2</sub>), and molybdenum disulfide (MoS<sub>2</sub>) [7,23–31] are among the examples of extensively reported inorganic nanofillers for polymer reinforcement. These nanofillers possess varieties of extraordinary properties like outstanding mechanical strength, high electrical and thermal conductivity, excellent friction and wear resistance, hydrophobicity, *etc.*, which lend a multitude of improvements to the properties of the reinforced polymers. There have also been studies on nanofiller derived from natural fibers such as wood dust, pinecone powder, jute, husk, mud, *etc.* [32].

The selection of the nanofiller is usually determined by the desired properties of the final nanocomposite.

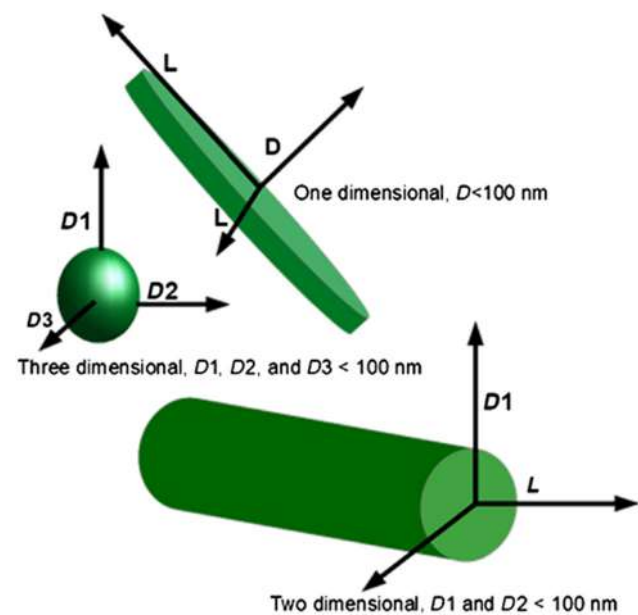


Figure 1: Size and morphology of different nanofillers [49].

Graphene and CNTs for instance are intrinsically electrically conductive, thus the nanocomposite incorporated by these nanofillers can be expected to be equipped with electrical conductivity properties. Although, the conductivity performance may be varied depending on the nanofiller distribution characteristics in the host matrix. There have also been reports that nanocomposites are usually more thermally stable [30,31,33] and chemically resistant [34–38]. However, generally, in cases where the nanofillers used were at their optimum concentration and good distribution and interfacial interaction between the fillers and the matrices were achieved, enhancements in the aspects of morphological, physical, and mechanical properties are the most commonly observed [31,32]. During mechanical loading, nanofillers can act as a stress transfer platform that distributes and minimizes the energy to slow down the crack propagation, which resulted in the improved mechanical performance of the nanocomposites.

Regardless of the remarkable intrinsic properties possessed by these nanoparticles, several factors like their dispersion in the polymer matrix, content, and also compatibility with the host matrix greatly determine their reinforcement performance. For example, homogenous nanofiller distribution in the matrix ensures sufficient interfacial interaction between the filler and the matrix, thus, delivering good compatibility. This is crucial in numerous nanofillers reinforcement enactment including stress transfer, conductive thermal and electrical pathways, active barrier properties, *etc.* However, many studies have reported increasing the content of nanofiller in the matrix led to poor nanofiller dispersion and agglomeration. Meanwhile, at low nanofiller content, the reinforcement performance is unsatisfactory [7,24–26].

One of the rising trends to address the drawbacks presented by single filler reinforcement is by incorporating a hybrid of different nanofillers into the polymer system. The hybrid of CNTs and NC [39], graphene and silver nanowire (AgNW) [40], SiO<sub>2</sub> and CNTs [41], graphene and CNTs [10,42–46], graphene and nanodiamond (ND) [47], and graphene and BN [22,48] are some of the examples of hybrid pairs that have been reported. These hybrids are usually designed based on their morphology and dimensionality, sizes, bonding mechanisms, and/or their inherent properties, according to the reinforcement needs of the polymer.

Over the years, many accounts have reviewed the performance and applications of nanofillers including hybrid nanofillers in various administrations. Figure 2 shows the progress and intermission in the works of the searching results of literature involving “nanofillers utilizations in polymer applications” in the past 5 years on

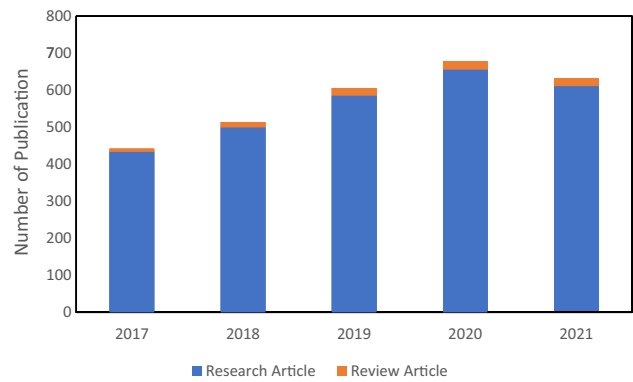


**Figure 2:** Chronological progress of nanofiller applications in literature in 5 years.

the Web of Science. The figure shows two categories of research which are the review articles and research articles. Of 2,872 articles, 85 of them are review articles, and the remaining 2,787 articles are research articles. The chronology shows an increasing trend in the research involving nanofiller in polymer applications. However, no kind of literature has covered a comprehensive review of the use of hybrid nanofiller systems in different thermoset and biothermoset applications.

In this study, we will discuss a general review of the synergistic reinforcement of hybrid nanofillers in selected recent publications on thermoset and biothermoset applications including electronic applications, thermal management, and barrier applications such as coatings and laminates, hydrogen storage, as well as biothermoset applications. The importance of synergistic hybrid interaction to improve polymer properties, as well as the factors influencing the synergic interaction between fillers will also be discussed.

## 2 Hybrid nanofiller

Hybrid nanocomposites have been reported to demonstrate greater improvements over conventional single nanofiller-reinforced composites. These improvements include increases in mechanical properties [25,29], better electrical and thermal conductivity [29], durable barrier performance, enhanced friction resistance [49], lower percolation threshold [43], *etc.* Among the reasons that produce these results is the improved dispersion of the nanofillers which leads to the synergistic interaction between the fillers and results in a unique interconnected 3D nanofiller network [40,43]. This provides an effective skeleton for mechanical support, broad protection for barrier performance, as well as

highly effective thermal and/or electrical conductivity. Furthermore, the combination of the different nanofillers in a single reinforcement system produces the communal properties of the fillers with dual effects. In several reports, hybrid nanofillers also balanced some undesired properties of certain fillers and generally result in better performance of the nanocomposites produced [50].

In various thermoset applications, these nanofillers' unique and intrinsic properties are cooperated and exploited to design and tune the finished properties required for the operations. Different nanofillers of diverse properties are hybridized to expand or level the properties of the other fillers to produce a synergistic performance. In electronic applications, for instance, the combination of two nanofillers with intrinsically high electrical conductivity leads to an extensive enhancement of the nanocomposite's conductivity owing to the improved nanofillers dispersion. This allows the nanofillers to exert their properties at the highest viable performance. Meanwhile, in the thermal management system, carbon-based fillers such as graphene nanoplatelets (GNPs) are often utilized due to their inherently high thermal conductivity. Hybridizing graphene with another thermally conductive filler with electrical insulative properties creates a hybrid system capable of thermal conductivity and concurrently electrically insulative which is practical for applications such as thermal interface material (TIM).

A multitude of other designs of the hybrid system can be generated based on these nanofillers manifold properties to be implemented in many other applications such as laminar and coating, hydrogen storage, *etc.* Table 1 summarizes the approaches that have been used for some of the thermoset and biothermoset applications and their advantages and limitations.

### 3 Synergistic hybrid nanofiller interaction in polymer nanocomposites

Synergistic hybrid interaction is one of the key defining factors that lead to the effectiveness of the hybrid nanofiller reinforcement performance. Several aspects influence their interaction including their content and ratio, morphology, and inherent properties. A synergistic filler combination leads to homogenous nanofillers distribution, reduces nanofillers agglomerations in the polymer matrix, and increases the interfacial interaction area with the host polymer. These often result in the formation of successfully augmented properties of nanocomposites

at low nanofiller content, which is one of the vital elements to ensure the material's lightweightness and cost-effectiveness.

Achieving an even nanofillers dispersion in the polymer matrix is one of the major challenges in the manufacture of nanocomposites. Nanofillers are exfoliated elementary layers or units from the stack of primary particles, generally in sizes ranging from 1–100 nm (Figure 3) [50]. These nanofillers are achieved by breaking down the primary particles' structure *via* several methods such as sonication, ball-milling grinding, chemical oxidation and reduction, *etc.* [40,66]. However, despite the techniques used, they tend to re-agglomerate in the polymer due to the strong Van der Waals force,  $\pi$ - $\pi$  interaction, or ionic bonding [67,68]. When they are added at high content, the forces intensify at close fillers' proximity, causing agglomeration.

Hybridizing different types of nanofillers has been reported to efficiently overcome this issue in numerous studies [39,67]. When two or more different nanofillers are combined in the polymer matrix, their interaction with each other results in the disruption of the forces that cause the nanofillers agglomerations. This interaction is usually termed nanofillers spacing or bridging (Figure 4) [12,69]. A continuous effect of this type of interaction builds the unique 3D hybrid nanofiller structures. In electronic and thermal applications, these 3D structures provide excellent pathways for electron and phonon transfer to enhance the conductivity of the nanocomposite. They also build a constant barrier from the penetration of aggressive elements and pronounced amelioration on the mechanical support of the nanocomposites such as the fracture toughness, tensile strength, and elasticity.

Additionally, a uniform hybrid nanofiller network increases the interfacial area between the nanofillers and the matrix. This provides an ample contact region for the stress transfer from the polymer to the fillers [12,33,68,70,71] that can produce a longer-lasting mechanical performance of the nanocomposites. For instance, a nanocomposite can deflect a crack from propagating further in the presence of nanofillers, thus, increasing its fracture toughness. During a tensile test, nanofillers restrict the movement and flow of the polymer chains and increase their elasticity and tensile performance.

Besides improving the interfacial interaction between the nanofillers and the matrix, the combination of nanofillers of different geometry also improves the interfacial compatibility among the fillers [72]. It usually leads to an increase in the contact area among the fillers and reduces their interfacial resistance. This is particularly important in the formation of uninterrupted channels for phonon and electron transport to ease and reduce the resistance

**Table 1:** Approaches, advantages, and limitations of hybrid nanofiller systems in selected applications

| Application                        | Approach  | Advantage  | Limitation   |
|------------------------------------|---|--|--|
| Electrical                         | Hybridizing two intrinsically high conductive nanofillers   | Better nanofiller dispersion, formation of the successive 3D network, lower electrical resistance, and lower percolation threshold [51–53]   | Creating a ratio of hybrid that produces enhancement in electrical conductivity properties with other properties such as thermal conductivity and mechanical properties                            |
| Strain sensing material            | Hybridizing a higher sensitivity nanofiller with a higher electrical conductivity nanofiller ( <i>e.g.</i> , GNP and CNT)<br>Hybridizing a higher conductivity filler ( <i>e.g.</i> , CNT) with other fillers | Increased sensitivity of the composites by the combination of piezoresistive behavior and tunneling transport mechanism [53–55]<br>Improved filler dispersion, improved filler network conductivity, and improved ability of the network to sense the rise in electrical resistivity [53–55] | Creating a hybrid system that provides a superior strain sensing ability and mechanical properties to support the longevity of the material  |
| Microwave absorbing material (MAM) | Hybridizing two intrinsically high conductive nanofillers<br>Hybridizing carbon-based filler with magnetic filler   | Improved filler dispersion, increased filler network conductivity, and increased RL loss [56]<br>Enhanced interfacial polarization, and improved impedance matching [57,58]  | Creating a single hybrid system that possesses a matching impedance  |
| Thermal management                 | Hybridizing a thermally conductive nanofiller with an insulative nanofiller   | Improved nanofillers dispersion created thermally conductive materials with insulated electrical conductivity [11,59]  | Ensuring a satisfactory thermal conductivity property of the hybrid system   |
| Barrier and tribological           | Incorporation of lubricative nanofiller in the hybrid system<br>Incorporation of inhibitive nanofiller in the hybrid system<br>Incorporation of insulative nanofiller in the hybrid system                    | Improved nanofiller dispersion, denser barrier network [35]<br>Formation of a passive layer that prevented the entrance of corrosive molecules [35,60]<br>Decrease in the nanofiller's network electrical conductivity, and prevention of galvanic corrosion of the material [60]            | Creating a hybrid system with a multi-performing ability for the coating applications  |
| Hydrogen storage                   | Hybridization of carbon-based nanofiller with metal-based nanofiller  | Improved nanofiller dispersion, increased interaction with hydrogen molecules, and increased hydrogen sorption [61–63]   | Creating a hybrid network with enhanced ability of hydrogen storage as well as superior mechanical properties to the polymer matrix to ensure the long-lasting utilization of the storage material |
| Bio-thermoset polymer              | Incorporation of hybrid nanofiller systems based on the application   | Ameliorated the reduced bio-polymer properties, particularly the mechanical properties [64,65]   | Creating a hybrid nanofiller system that can provide sufficient improvement and amendment to the bio-thermoset polymer   |

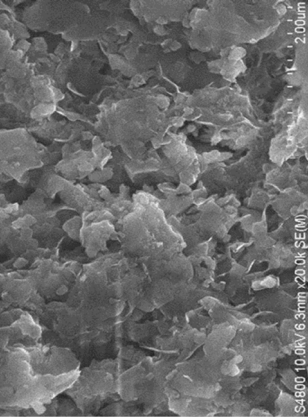
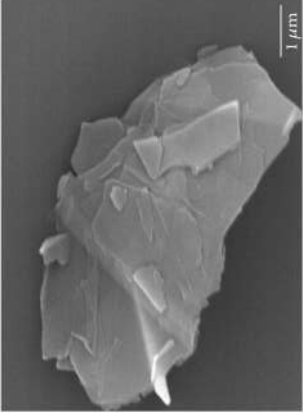
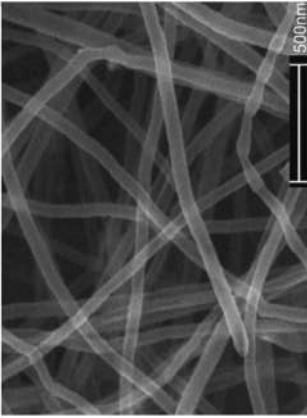
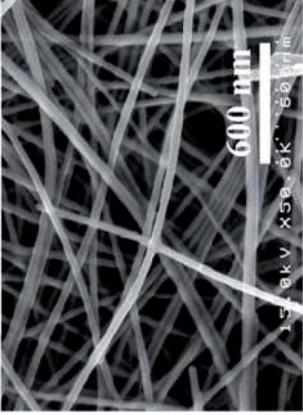
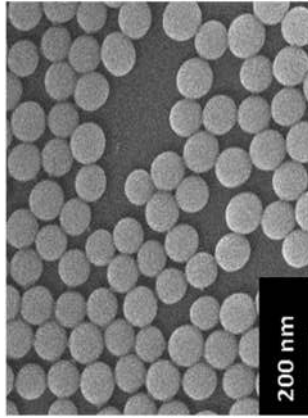
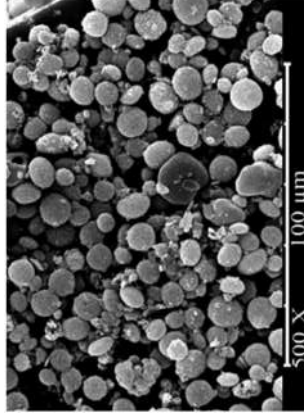
of the conductivity. Furthermore, the consistent filler dispersion can effectively lower the nanofillers' percolation threshold while simultaneously producing an improved conductivity [13,41].

Synergistic interaction between hybrid nanofillers also results in the effective magnification of the properties of the nanocomposites through the joined effect of the intrinsic properties of the fillers [71]. Moreover, the

improvement in the dispersion of the fillers also leads to a massive enhancement of the quality of the nanocomposites even at a lower filler loading [56,57]. On the other hand, synergistic hybrid filler distribution also allows the addition of a higher filler loading with little hazard of filler agglomeration [71].

Besides amplifying the properties, studies have also shown that hybridizing different nanofillers can efficiently

**Table 2:** SEM images of different dimensionality nanofillers

| Dimensionality | Nanofiller  |
|----------------|---|
| 1D             | <p data-bbox="284 1464 304 1564">MMT [80]</p>  <p data-bbox="284 676 304 776">GNPs [81]</p>             |
| 2D             | <p data-bbox="632 1464 652 1564">CNTs [82]</p>  <p data-bbox="632 661 652 776">AgNWs [83]</p>           |
| 3D             | <p data-bbox="979 1412 1000 1564">Nanosilica [84]</p>  <p data-bbox="979 697 1000 776">CB [85]</p>  |

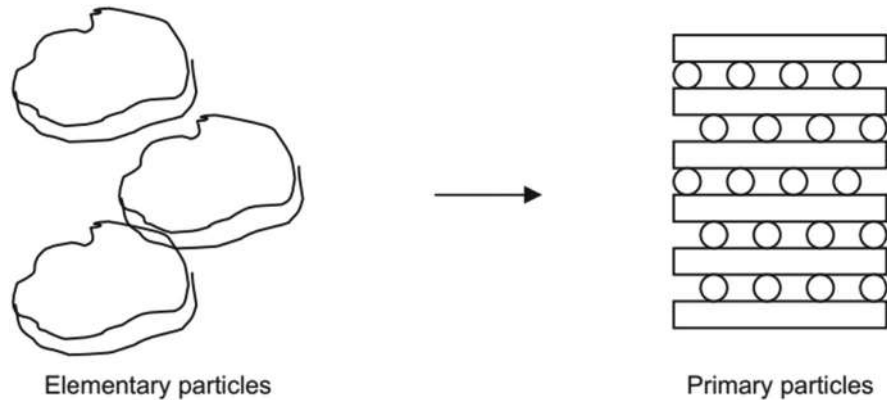


Figure 3: Schematic illustration of elementary and primary particles [50].

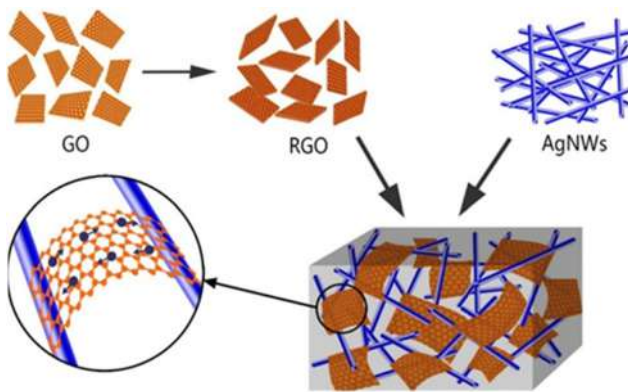


Figure 4: Bridging effect between RGO and AgNWs [74].

balance some undesired properties of the nanofillers for certain applications [73]. For instance, combining two thermally conductive nanofillers while one of the fillers is also electrically insulative can produce a nanocomposite with enhanced thermal conductivity, yet electrically insulated for an effective application in thermal insulating materials.

### 3.1 Factors determining the hybrid synergistic effect

Several factors affect the nature of the interaction between the hybrid nanofillers. The nanofiller morphologies including their size, dimensionality, and orientation can significantly regulate the contact between the different morphological fillers. For instance, one-dimensional (1D) nanofillers such as montmorillonite (MMT) and GNPs are usually in the form of sheets and provide excellent interfacial contact with the host polymer and with the other fillers [49]. Two-dimensional (2D) nanofillers such as CNT and AgNWs can be hybridized with the 1D fillers

to form a bridge between the 1D sheets. This will construct a connected hybrid 3D network with continuous contact between the fillers and the fillers with the polymer matrix [12,75]. Spheric and cubic three-dimensional (3D) nanofillers such as nanosilica, nanoalumina, polyhedral oligomeric silsesquioxane (POSS), and carbon black (CB) have also been hybridized with 1D and 2D nanofillers [11,76]. Table 2 shows the scanning electron microscope (SEM) images of some of the examples of different nanofillers of different dimensionality. Figure 5 shows the schematic diagram of the hybrid combining nanofillers of different dimensions (1D GNPs, 2D AgNWs, and 3D SiO<sub>2</sub>) [11].

Furthermore, the optimum content and ratio of the hybrid are also substantially affected by the nanofiller structure and morphology. These two factors can greatly influence the interaction of the nanofillers and determine the hybrid network it produces. Ranging results have been reported for identical hybrids when different content and ratio of the hybrids are used [77]. Additionally, the methodology used to disperse the nanofillers also produces a significant impact. Several different techniques have been reported to enhance the dispersion of the nanofillers and the results are still varied even with identical filler content and ratio [51,78].

The usage of hybrid nanofillers with varied and balancing properties is also effective to produce synergistic interaction of nanofillers for amplified and/or complementary advanced properties for polymer applications. Hybridizing highly electrically conductive carbon nanofillers such as CNT and GNP can build an amplified conductive network. This enhancement in conductivity is due to the coupling effect of the nanofillers and better CNT and GNP dispersion which improved the electron transfer channel [79]. On the other hand, the addition of POSS nanofiller to graphene can efficiently reduce the electrical conductivity of graphene. Simultaneously,

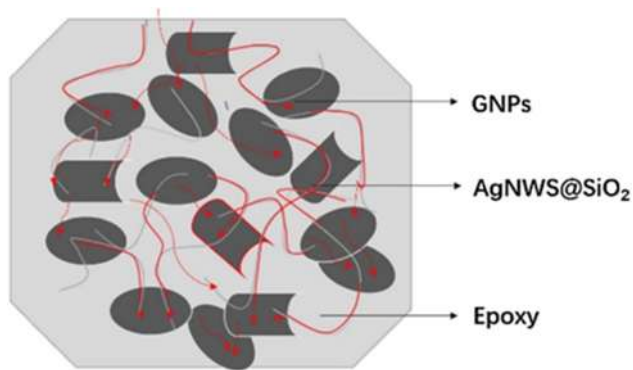


**Figure 5:** The schematic diagram of the hybrid GNPs/AgNWS/SiO<sub>2</sub> thermal conductive network [11].

it also maintains and intensifies the efficiency of graphene for shielding performance in the application of coating performance [60].

## 4 Hybrid nanofiller in electronic applications

Recent years have seen vigorous developments in electronic inventions including miniaturization, increased power density, and higher performance of integrated circuits. This advancement compels a series of enhancements of the merchandise covering higher electrical conductivity, better thermal management systems, improved management

of electromagnetic (EM) pollution, *etc.* Nanofillers such as CNT, graphene, CB, NC, ferrite, ND, *etc.*, have been abundantly used as electrically conductive fillers due to their lightness, ready accessibility, excellent conductivity, physical and chemical characteristics, and dielectric and EM properties [51,52,56,58,86].

Among these nanofillers, carbon nanofillers particularly CNT is commonly used owing to their extremely high inherent electrical conductivity ( $10^6$ – $10^7$  S/m). Hybridizing CNT with other nanofillers results in better CNT conductivity performance due to better dispersion of the nanofillers in the polymer matrix. This results in the formation of successive network structures with lower resistance for electron transfer channels at a lower percolation threshold [51–53].

The hybrid of CNT and GNP is frequently reported in the studies of electrically conductive polymer applications. Their plane arrangement of hexagonal C–C covalent bond provides an excellent path for electrical conductivity. In the formation of the CNT/GNP conductive network, the tubular-structured CNTs correspond to the micro-sized *z*-direction, meanwhile GNPs nanosheets in the planar form contest to the *XY*-plane. During the electrical conduction, the CNTs conductivity network preferably occurs in their *z*-direction. The GNPs network on the other hand delivers the electrical contacts between nanosheets in a perpendicular direction. This results in denser electrical connections of the *XYZ* network, thus easing and augmenting the conductivity (Figure 6) [51,87,88].

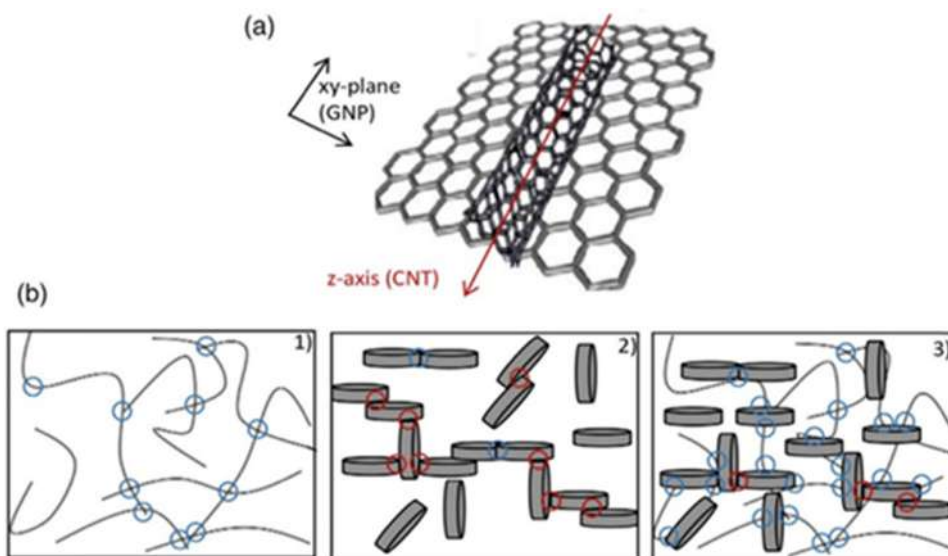


**Figure 6:** (a) The *XYZ*-plane directions of the hybrid CNT/GNP electrical transport. (b) (1) CNT network electrical contacts, (2) GNP, and (3) hybrid CNT/GNP electrical contacts. The blue colors show the electrical contacts with less resistance than those indicated by the red colors [88].



A study by Li *et al.* [52] demonstrated an example of the synergistic effect of the hybrid CNT/GNP in electrical and thermal conductivity. They reported a substantial lessening in the epoxy (EP)-based carbon fiber-reinforced plastics (CFRPs) laminate (for the application in lightning strike protection and EM shielding) surface electrical resistivity when a hybrid of CNT/GNP was incorporated. The resistivity lowered by four orders of magnitude, from 2–3  $\Omega/\text{sq}$  (CFRPs) to  $3 \times 10^{-4} \Omega/\text{sq}$  with the incorporation of the hybrid CNT/GNP. Meanwhile, for CNT-only coating, the surface electrical resistivity was lesser compared to the hybrid coating ( $1.03 \times 10^{-3} \Omega/\text{sq}$ ). The thermal conductivity on the other hand amplified more than seven times, from 200 to 1,500 W/m K.

The reason for the much lower resistivity in the hybrid composites was due to the formation of 3D conductive networks of 1D CNTs and 2D GNPs. The tubular form of CNTs bridged the adjacent GNP sheets, hindering the nanosheets from agglomerating and improving the nanofillers' dispersion in the matrix. This allowed the use of the large nanofillers' specific surface area to their highest extent and lengthen the conductive pathways that resulted in the increased conductivity of the composites.

A similar synergistic effect of 1D CNTs bridging 2D GNPs has also been reported by Caradonna *et al.* [51]. However, in this study, they also described the dominating role of CNTs in the electrical conductivity performance of the composites due to the higher intrinsic electrical conductivity of CNTs ( $10^6 \text{ S/m}$ ) compared to GNPs ( $10^5 \text{ S/m}$ ). The studies showed that further increasing the content of GNPs of the hybrids did not produce any significant changes in conductivity. Although, at different CNT concentrations (0.1 and 0.05 wt%), the ratios of the CNT/GNP that produced the best conductivities were different (1:10 and 1:40). This showed that the contents and ratios of the hybrids are among the crucial factors that determine the performance of the composites. Moreover, this study also highlighted the importance of nanofillers dispersion methods and their optimization to produce an ideal hybrid distribution and interaction. In this study, an optimized calendaring process using a three-roll mill operation was used to produce a distribution of nanofillers in the preferred orientation to aid a better conductivity based on the orientation's direction.

The synergistic interaction between the hybrid of CNT/GNP was noticeably demonstrated by a significant lowering of the percolation threshold when the hybrid was employed. At 0.1 wt% multiwalled carbon nanotube (MWCNT) loading, the nanocomposite retained similar conductivity to the neat EP ( $<1 \times 10^{-9} \text{ S/m}$ ). Similarly, when GNP was incorporated in loadings ranging from

0.5 to 5.0 wt%, there was also no change observed in the conductivity. However, when 0.1 wt% MWCNT and 2.0 wt% GNP were combined, the conductivity increased substantially by six orders of magnitudes ( $1.32 \times 10^{-3} \text{ S/m}$ ). In the single-filled nanocomposites, similar conductivity was only achieved by MWCNT at 0.4 wt% loadings ( $5.08 \times 10^{-3} \text{ S/m}$ ), and GNP at 20.0 wt% loading ( $2.14 \times 10^{-4} \text{ S/m}$ ).

Han *et al.* [87] have also reported the effectiveness of employing the hybrid of CNT and GNP to improve the performance of the electrical conductivity of the composites. Besides facilitating a homogenous dispersion of the nanofillers, they have also described that the addition of GNPs to CNTs helped to prevent damage to CNTs during the processing. This helped to preserve the length and rigid structure of CNTs for better electrical conduction and also to provide better bridges to fill the gaps between GNP platelets for the formation of a 3D hybrid electron conductive path.

A significant reduction in the electrical percolation threshold of the hybrid nanocomposites was recorded. Although the conductivity of the GNP-EP, CNT-EP, and the hybrid GNP/CNT-EP nanocomposites were roughly comparable ( $\sim 10^{-5} \text{ S/m}$ ), the hybrid nanocomposites recorded a much lower percolation threshold at 0.41 vol%, which was 29.3% lower than the nanocomposites of GNP-EP, and 22.6% lower than the CNT-EP nanocomposite.

Additionally, the hybrid nanocomposites also demonstrated outstanding improvements in mechanical performance. This was due to the enhanced dispersion of the nanofillers and the formation of 3D hybrid networks which lead to the increased interfacial contact area between the nanofillers and the matrix which promoted the load transfer, stress concentration, and defect distribution. The Young's modulus, toughness, and lap shear strength of the hybrid nanocomposites were reported to increase by 89, 113, and 98% over the neat EP.

Based on these studies, it can be concluded that the implementation of CNT and GNP as hybrid nanofiller reinforcement to improve the electrical conductivity of composites is more effective than implementing CNT or GNP alone. The presence of CNTs helps to bridge the GNP platelets, thus preventing the restacking of the platelets. Meanwhile, the presence of GNPs can help to uncurl and align the CNT structures to their proper length. These two mechanisms show the compatibility of CNT and GNP as hybrid fillers to facilitate the configuration of the 3D conductive networks which is exceptionally crucial for ease and increased electrical conductivity.

Nevertheless, these studies also showed that the preparation methods, as well as the contents and ratios of

the nanofillers, greatly influenced the electrical conductivity performance of the nanocomposites. Thus, further comprehensive research must still be carried out to find out the relationship between these factors. Furthermore, when regarding these nanocomposites for industrial applications in electronic sectors, an extensive analysis of the effects of the hybrid fillers on other properties such as thermal conductivity and mechanical performance must also be conducted.

## 4.1 Strain sensing materials

In the electronic application for strain sensing materials such as non-destructive testing materials, guided lamb waves, optical fibers, capacitive pressure sensors, structural health monitoring, *etc.*, the defects and failures are detected through the analysis of the electrical fluctuations in the nanofillers electrical percolation network. These fluctuations are caused by the network distortion that results from the strain or cracking of the repetitive movements or applied pressure [54,89]. The strain applied to the nanocomposite materials causes resistance in the electron tunneling transport between the adjacent nanofillers. Additionally, the inherent piezoresistive behavior of the nanofillers detects the rise in the electrical resistance caused by the disruption of the electrical network [53–55].

The effectiveness of strain sensing application depends greatly on the conductivity as well as the sensitivity of the nanofillers network in the nanocomposite. The 2D planar morphology of GNP provides a large interparticle distance between the neighboring fillers, thus demonstrating greater sensitivity to detect electrical resistance. CNT on the other hand is higher in intrinsic electrical conductivity and able to deliver better conductivity at a lower percolation threshold [53,78,90–92]. Hence, hybridizing GNP and CNT can deliver a strain sensing network of superior conductivity and sensitivity. Nevertheless, apart from the compatibility of the CNT/GNP hybrid, other factors including the dispersion method, the nanofiller contents, and the nanofiller ratios also substantially influence their sensing properties.

Sanchez-Romate *et al.* [53] studied the effect of employing the hybrid GNP/CNT at ranging ratios and different dispersion methods on the behavior of the sensing aptitude of the nanocomposites. The study demonstrated differences in conductivity when different sonication times were employed on the nanofillers. Here they discussed the effectiveness of the sonication process in the nanofiller's exfoliation depending on the viscosity of the medium. Hence, at a higher nanofiller concentration, the viscosity of the

medium increases, thus a longer sonication time is needed to achieve a good filler dispersion. However, at a lower filler concentration, the viscosity of the medium decreased, hence employing a similar sonication time would cause damage to the nanofiller. The damage would lower the specific surface area of the nanofiller and also lead to a lowering of the composite's conductivity.

Compared to GNP, the effect of the sonication times showed more influence on CNTs. At lower CNT and GNP contents (0.1 and 5 wt%), the viscosity of the medium was lesser, thus, a 30 min sonication time of CNT resulted in an excessive cavitation force that caused damage to CNT and reduced its specific surface area. These led to an increase in the percolation threshold of the hybrid network. Regarding the sensing aptitude of the hybrid, an increase in the percolation threshold led to an increase in the interparticle distance and promoted a more dominant tunneling effect, and improved the sensitivity of the nanocomposites.

However, regardless of the dispersion methods and the conductivity of the nanocomposites, their sensing performance was influenced more by the nanofiller contents and types. In the nanocomposites with a higher GNP ratio, the electrical pathways were dominated by the role of GNP. This resulted in a recurrent exponential behavior of the electrical resistance with the applied strain with recorded gauge factors (GFs) of the GNP/CNT hybrid of 5 wt% GNP and 0.1 wt% CNT reaching  $\sim 10$ . On the other hand, when the content of the CNT in the hybrid was increased to 0.2 wt%, the formation of the electrically conductive network was dominated by CNT. Thus, a more linear response was observed due to the higher frequency of the tunneling transport mechanism of CNT, with GFs reaching  $\sim 4$  (Figure 7) [53].

Similar piezoresistive behavior of hybrid nanocomposite was also reported by Esmaili *et al.* [67]. However, in this study, only the CNT was introduced to the composites to induce electrical conductivity and piezoresistive behavior, while NC was added to facilitate the dispersion of CNT for better conductivity and to further improve the fracture toughness of the nanocomposites. Although CNT was the only nanofiller in this hybrid system with the intrinsic aptitude for electrical conductivity, a considerable enhancement in the conductivity was observed compared to the composites containing only CNT. This was due to the enhanced dispersion of CNT in the presence of NC which increased the number of electrical networks formed.

The conductivity of the hybrid nanocomposites containing 1 and 0.5 wt% of NC increased by 400 (0.05 S/m) and 700% (0.08 S/m) over the CNT–EP. Correspondingly,

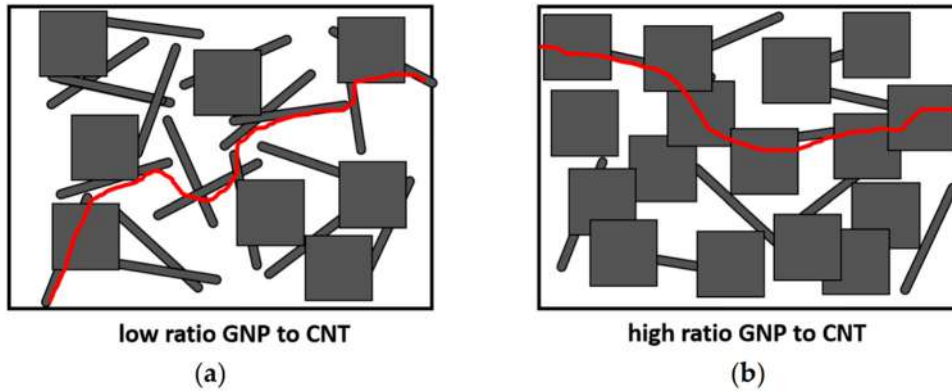


**Figure 7:** Favorable conductive pathways with different GNP to CNT ratios: (a) low ratio GNP to CNT and (b) high ratio GNP to CNT [53].

the piezoresistive properties were improved in the hybrid nanocomposites. The CNT–EP piezoresistive behavior was dominated by the tunneling resistance of CNT. Meanwhile, the enhancement of the conductivity network in the hybrid EP also led to the loss of the electrical contacts between the neighboring CNTs in addition to the CNT tunneling transport mechanism. This resulted in the largely increased sensitivity of the hybrid nanocomposite. Consequently, the sensitivity of the hybrid nanocomposites improved by 30 and 13% at  $\varepsilon \sim 0.01$  compared to the CNT–EP nanocomposite (1.53).

Furthermore, the mechanical performance of the EP nanocomposites was also greatly enhanced by the implementation of the hybrid CNT/NC. The addition of NC acted as a hurdle to prevent CNT agglomeration and improved the dispersion of CNT in the EP matrix. This subsequently led to improved interfacial bonding of the nanofillers with the matrix. The synergistic effect of the hybrid was well demonstrated in the improved fracture toughness of the EP composites. The improved dispersion of the hybrid in the matrix led to better crack deflection and crack bridging. During crack deflection, the crack front would split into micro cracks and be dispersed around the nanofillers. This deflection resulted in further dissipation of energy which required a higher amount of energy for the cracks to propagate further.

The assessment of the mechanical properties of strain sensing nanocomposites is especially important particularly to ensure the longevity of the strain sensing application. Strain sensing materials are subjected to constant strain and pressure, thus developing a material that can sustain stability and sensitivity through repetitive cycles of mechanical stress is vital.

For instance, in a study conducted by Guo *et al.* [54], they tested furfurylamine (FA)-functionalized dynamic covalent bismaleimide (BMI) cross-linked poly (butylene sebacate-co-butylene fumarate) (PBSF) (PFB) nanocomposites

for three types of strain-sensing applications: a triboelectric nanogenerator, a capacitive pressure sensor, and a flexible keyboard. In this study, self-healing was one of the key properties that should be possessed by the nanocomposites. Thus, besides owing good electrical and piezoresistive properties, the nanocomposites must also have good mechanical properties.

In this study, CNT, silver nanoflakes (AgNFs), and CB were introduced into PFB as the hybrid nanofiller. 1D CNTs acted as the backbone of the network, while the 2D AgNFs made the contact junction between the CNT networks to prolong the conductivity path. CB on the other hand filled the interspace of the AgNFs/CNTs mesh, building a unique 3D nanofillers network for mechanical support and electrical conductivity pathways. The nanofillers-filled PFB composites (PFBC) showed better mechanical properties compared to the neat PFB. The tensile strength increased by 66.7% ( $\sim 5$  MPa), the maximum elongation was retained at  $>350\%$ , and after three recycles, the conductivity and the toughness were maintained at 100 S/m and  $10.1 \text{ MJ/m}^3$ . After  $\sim 3,000$  consecutive cycles, the electronic materials preserved stable structural integrity and sensing reliability performance.

From these summarized studies, it is evident that CNT plays a major role in generating the electrical conductivity and piezoresistive characteristics of thermoset nanocomposites. However, it is also worth noting that the presence of another nanofiller in the CNT-hybrid systems considerably improve the reinforcement performance of CNT. The enhancement in the nanofillers' dispersion when hybrids are implemented is the primary factor that leads to these improvements with significant results in lowering the percolation threshold and higher sensitivity of the nanofillers network.

Although, as has already been discussed in previous sections, and also demonstrated in these studies, the

compatibility and synergistic interaction between hybrid fillers are substantially determined by the elements such as dispersion methods and parameters, nanofiller types and characteristics, and their content and ratio. Based on these studies, it could be gathered that by combining different types of nanofillers at certain contents and ratios and employing varying dispersion methods, the desired 3D conductive networks could be achieved, nonetheless at ranging levels of performance. Thus, these aspects must be thoroughly studied to allow a comprehensive understanding of the subject of hybrid nanofiller's conductivity and the strain-sensing ability for future applications.

## 4.2 Microwave absorption material

High-performance MAM is another growing development of electronic applications in advanced polymeric materials due to the evolution in the use of EM wave communication and stealth technology such as in defense and military. Besides, the progression of the performance of other electronic applications also results in the increased emission of EM pollution. MAMs are developed principally to resolve the problems of EM compatibility and EM pollution by generating EM interference through the conversion of the absorption energy of EM incident energy into other forms like the heat of low intensity and low return loss (RL). Lightweight materials, with broad bandwidth below  $-10$  dB, strong consumption capacities, and tunable absorption frequency are among the desired characteristics for the advanced applications of MAMs [56,58,93–100].

The microwave absorption performance of material relies significantly on the impedance matching condition of the composites. To produce a good impedance matching, the input impedance ( $Z_{in}$ ) and the corresponding attenuation constant ( $\alpha$ ) must conspire accordingly [56,58,93,94,101,102]. When the impedance of a composite is closed to that of a vacuum ( $377 \Omega$ ), the EM wave can penetrate easily through the materials. Subsequently, a high attenuation constant leads to a good absorption performance of the permeated wave [56]. Additionally, the impedance matching degree is influenced by the complex permittivity; meanwhile, the complex permittivity is determined by the dielectric and EM properties of the composites which are significantly regulated by the dispersion, content, and the networks conformation of the nanofillers in the polymer matrix [56].

The study by Liu *et al.* [56] demonstrated the effect of nanofillers' dispersion, contents, and conductive network distributions on the EM absorption performance of the

hybrid nanofillers. In this study, they created a porous structure of EP composites reinforced with GO–CNTs hybrid for microwave absorbers application. The porous layout of the composites reduced the density of the materials and improved the absorption performance by increasing the multi-reflecting and scattering numbers. Solid CNT–EP composites and porous CNT–EP composites of similar contents as hybrid composites were also prepared for comparison.

The solid composites should have a better performance compared to the porous composites due to the low number of effective CNTs in the porous structure to build the conductive networks. However, it is worth noting that at similar nanofillers' content (3.0 wt%), the hybrid GO–CNT foam structure achieved comparable values of the real ( $\epsilon'$ ) and imaginary ( $\epsilon''$ ) permittivity (55 and 81) to the solid CNT–EP composites (54 and 84). On the other hand, the  $\epsilon'$  and  $\epsilon''$  values of CNT–EP foam were considerably lower (38 and 40) at a similar concentration.

These improvements were due to the addition of GO to CNT which improved the nanofillers' dispersion and overcame the problem of poor CNT conductive networks in porous materials. The conductivity of the hybrid nanocomposites also improved up to 71.4% (18 S/m). These improvements led to a considerable performance of the RL which attained a value of  $-20$  dB with a  $-10$  dB range of 5.3 GHz (10.8–16.1 GHz). To enhance the absorption potential further, multi-layered structures of the impedance layer and absorption layer were created. A 2 mm thick foam structure of 0.5 wt% GO–CNTs/EP was combined with 1 mm thick 2.0 wt% GO–CNTs/EP to produce a MAM with an RL value of  $-40$  dB with a  $-10$  dB range of 7.1 GHz (9.9–17 GHz).

Nanofillers such as CB, CNT, and graphene [94,103–106] possess novel dielectric loss characteristics and can lead to a substantial leap in RL values. Nevertheless, incorporating a single component of these fillers can only yield a limited extent of improvement in the absorption properties of the nanocomposites. This is due to the impedance mismatch that usually results from the improper conductivity within the interface of air/absorbers and the single loss mechanism which restricts their upper limit of RL values. According to Maxwell–Wagner–Sillars theory, hybrid components have improved interface polarization due to the induced charges at the interfaces of the components under applied alternative EM field, hence producing a material with better dielectric loss [57,107]. Thus, several studies have reported the hybridization of carbonaceous nanofillers with magnetic nanofillers such as metallic iron (Fe), hexagonal and spinel ferrites, nickel (Ni) [95,108], *etc.*, could enhance the microwave absorption properties.

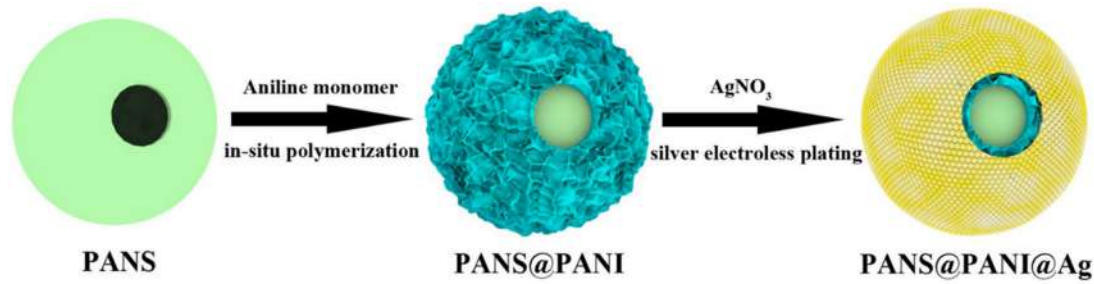


**Figure 8:** Synthetic way of the production of PANS@PANI@Ag hybrids [57].

For instance, the study by Zhang *et al.* [57] showed the synergistic effect of adding RGO sheets to the conductive microsphere of PANS@PANI@Ag to enhance the microwave absorption properties of EP nanocomposites. Initially, Ag nanoparticles were attached to the hollow double-shell of poly(acrylonitrile) microspheres@polyaniline (PANS@PANI@Ag) (Figure 8). The addition of the Ag layer led to a considerable increase in the hybrid structure conductivity due to the PANI network being already electrically conductive. This resulted in a very high conductivity that produces an eddy current on the surface and causes the incident microwave to reflect rather than enter the materials. This creates an impedance mismatch and weakens the performance of the microwave absorption of the nanocomposites.

The addition of RGO to the PANS@PANI@Ag structure further enhanced the conductivity of the nanofillers network (Figure 9). However, the inherent dielectric properties of RGO, as well as its remaining defects and residual groups, contributed to defect dipole polarization, interfacial polarization, and appropriate conductive loss proposed by

the Maxwell–Wagner–Sillars theory. These led to better impedance matching with  $\sim 90\%$  attenuation of incident microwave energy of the hybrid nanocomposites. An optimal RL of  $-44.9$  dB at  $9.16$  GHz with corresponding effective bandwidth of  $\sim 2$  GHz was achieved by the EP composites filled with  $1$  wt% RGO and  $1$  wt% PANS@PANI@Ag.

A similar author has also conducted a study on the microwave absorption properties of EP composites reinforced with (Ni) and RGO [58] (Figure 10). In this hybrid system, the improvement of the absorption performance of the composites was achieved through several mechanisms. First, the decoration of hollow microspheres Ni shell on the surface of RGO helped to produce a uniform distribution of RGO inside the EP matrix (Figure 11). This then resulted in the formation of an effective RGO conductive network. Second, the magnetic properties of Ni led to an enhanced magnetic loss and restrained the formation of eddy current which came from the high conductivity of RGO networks. Additionally, the dielectric properties of RGO and the defects and residual groups of RGO further contributed to the dielectric loss. Ultimately, the combination of the

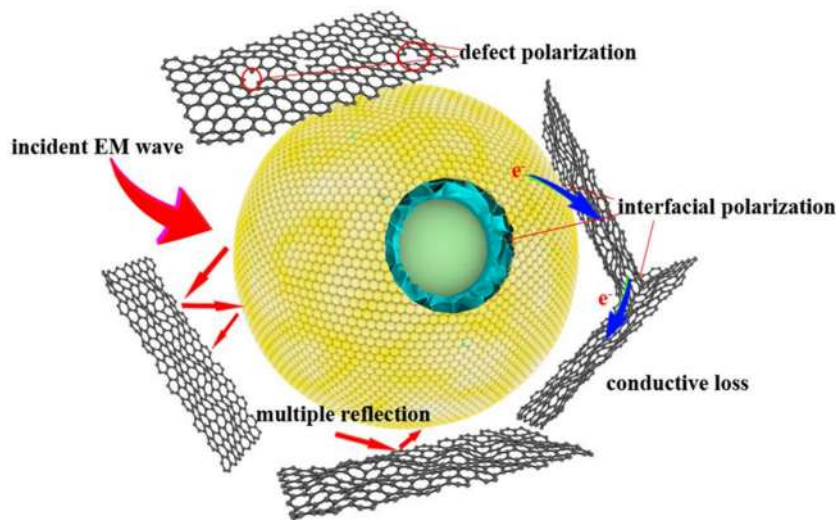


**Figure 9:** The illustrative of the microwave absorption system of RGO–PANS@PANI@Ag/EP composites [57].

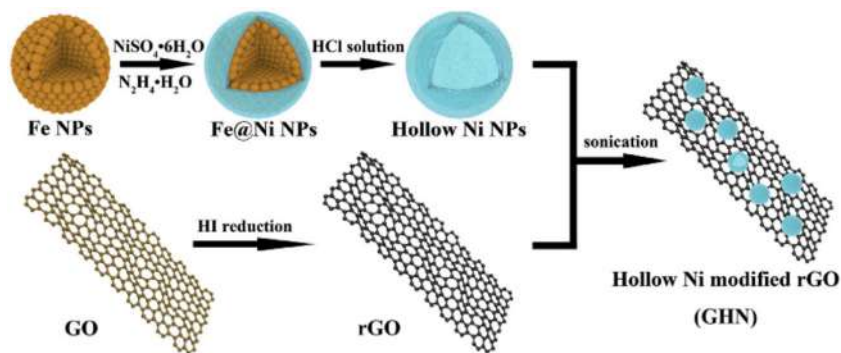


**Figure 10:** The synthetic route of the development of hollow Ni-modified RGO composites [58].

different fillers created an enhanced interfacial polarization which then improved the impedance matching and resulted in a higher attenuation constant for a better absorption performance. A minimum reflection loss of  $-33.1$  dB at  $4.4$  GHz was achieved at the matching thickness of  $4.9$  mm when  $1$  wt% of RGO and  $10$  wt% of hollow Ni were incorporated.

The reviewed studies show the significance of employing hybrid nanofiller systems to achieve satisfactory microwave absorption properties of nanocomposites. Despite a high intrinsic electrical conductivity and dielectric properties of a nanofiller, many other factors such as nanofiller dispersion, impedance matching, attenuation constant, interfacial polarization, *etc.*, require the incorporation of other compatible fillers to attain the desired absorption properties. Similar to strain-sensing properties, microwave absorption properties involve a complementary relationship of excellent electrical conductivity with appropriate impedance matching. Hence, finding a suitable complementary nanofiller is vital in designing this hybrid system.

Tables 3 and 4 summarize the properties of the hybrid nanocomposites for the electronic applications that have been discussed in this section. It can be concluded that hybridizing nanofillers of appropriate types, ratios, and intrinsic properties can produce a better performance of varying properties for polymeric applications in electronic sectors.

## 5 Hybrid nanofiller in thermal management applications

The development in electronic applications such as greater speed, portable size, lighter, higher power circuit, higher voltage EM environment, *etc.*, leads to the accumulation of heat flux that is destructive to the operation and integrity of the materials. Hence, to guarantee the longevity of their

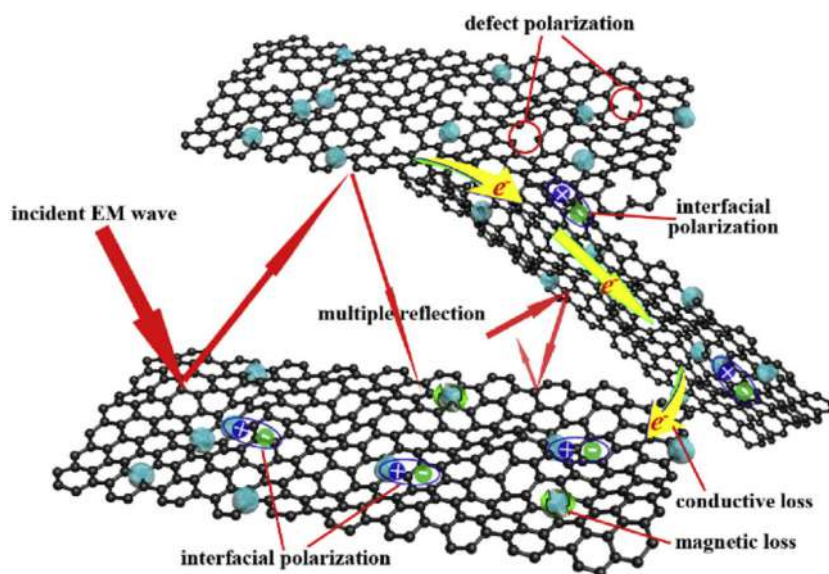


**Figure 11:** The illustrative diagram of the microwave absorption system of hollow Ni-modified RGO composites [58].

Table 3: Hybrid nanocomposite properties for electronic applications

| Matrix        | Hybrid       | Application               | Electrical conductivity (S/m)                  | Electrical resistance ( $\Omega/\text{sq.}$ ) | GF         | Thermal conductivity (W/m K)           | Young's modulus (GPa) | Tensile strength (MPa) | Lap shear strength (MPa) | Reference |
|---------------|--------------|---------------------------|--|---|------------|--|-----------------------|------------------------|--------------------------|-----------|
| EP-based CRFP | CNT/GNP      | LSP, EIM shielding        | Not stated                                     | $3 \times 10^{-4}$                            | Not stated | 1,500                                  | Not stated            | Not stated             | Not stated               | [52]      |
| EP            | CNT/General  | General                   | $6.02 \times 10^{-5}$ to $1.32 \times 10^{-3}$ | Not stated                                    | Not stated | $0.231 \pm 0.006$ to $0.475 \pm 0.005$ | Not stated            | Not stated             | Not stated               | [51]      |
| EP            | CNT/General  | General                   | $\sim 10^{-5}$                                 | Not stated                                    | Not stated | Not stated                             | 2.25–2.75             | 34–51                  | $17 \times 10^{-23}$     | [87]      |
| EP            | GNP/GNP/CNT  | Strain sensing            | $\sim 3 \times 10^{-3}$                        | Not stated                                    | 3–10       | Not stated                             | Not stated            | Not stated             | Not stated               | [53]      |
| EP            | CNT/NC       | Strain sensing            | 0.05 to 0.08                                   | Not stated                                    | 1.7–2.0    | Not stated                             | Not stated            | $\sim 60$              | Not stated               | [70]      |
| PFB           | CNT/AgNFs/CB | Recyclable strain sensing | 100  | Not stated                                    | Not stated | Not stated                             | Not stated            | $\sim 5$               | Not stated               | [54]      |

performance, a superior thermal management system must be considered and implanted.

Carbon-based nanofillers such as CNT and graphene, metal nitrides such as BN, aluminum nitride (AlN), and silicon carbide, metal oxides such as aluminum oxide ( $\text{Al}_2\text{O}_3$ ), magnesium oxide (MgO), and organo-montmorillonite, and metallic fillers such as Ag, copper (Cu), and Al are among the fillers that possess superior thermal conductivity [11,47,48,66–69,71,73,108]. Besides, these fillers also have excellent mechanical strength, thus, hybridizing these fillers not only produces a material with superior thermal conductivity but it is also equipped with durable mechanical properties for a long-lasting application.

The specific surface area of a nanofiller is one of the important factors in a composite material that affects the chemical and physical aspects of the composite. A higher specific surface area means a higher interfacial interaction per unit volume with the polymer matrix [47]. During thermal conduction, a good nanofiller distribution provides sufficient interfacial contact between the filler and the matrix for efficient heat dissipation and prevents the occurrence of heat flux on the surface of the composite. Nanofiller's agglomeration reduces their specific surface area, hence providing insufficient contact to interact with the matrix.

Combining compatible hybrid nanofillers have been numerous reported to facilitate a homogenous dispersion of the nanofillers, thus resulting in a hybrid structure with a higher specific surface area. A study conducted by Zhang *et al.* [47] has shown that when GNPs were hybridized with ND, the presence of ND promoted the exfoliation of GNPs, resulting in good dispersion of the hybrid ND@GNPs in the EP matrix. The specific surface area of the hybrid structure increased to  $58.6 \text{ m}^2/\text{g}$ , which was a 69.9% improvement from the exfoliated GNPs structure.

Additionally, a homogenous nanofiller dispersion is also vital in building an effective conductive network for phonon transfer. After the heat is transferred from the matrix to the filler, a good conductive network provides a consistent pathway for phonon transfer and increases the thermal conductivity of the nanocomposite. In this study, they reported an enhancement of 1,205% (2.48 W/m K) of the thermal conductivity of EP nanocomposites when incorporated with the hybrid GNP and ND. During the surface temperature variation over time test, the EP nanocomposites containing hybrid ND@GNPs heated the quickest with a temperature close to  $90^\circ\text{C}$  after just 100 s. These results indicated the superiority of the thermal conductivity properties of the hybrid network due to their homogenous distribution inside the polymer matrix.

**Table 4:** Microwave absorption properties of hybrid nanocomposites

| Matrix | Hybrid | Real part ( $\epsilon'$ )<br>permittivity | Imaginary part ( $\epsilon''$ )<br>permittivity | Conductivity<br>(S/m) | Attenuation<br>constant (1/m) | Reflection<br>loss (dB) | Reference |
|--------|--------|---|---|-----------------------|-------------------------------|-------------------------|-----------|
| EP     | GO/CNT | 55  | 81  | 18                    | 800                           | -15 to -40              | [56]      |
| EP     | Ag/RGO | 26.4                                      | 12  | Not stated            | 600                           | -18.9 to -44.9          | [57]      |
| EP     | Ni/RGO | 15  | 3.4   | Not stated            | 210                           | -23 to -33.1            | [58]      |

Furthermore, the uniform hybrid nanofiller dispersion and the network conformation also contributed to enhanced mechanical properties of the nanocomposites. The 3D nanofiller formation and substantial interfacial contact between the nanofillers and the matrix restricted the polymer chain motion. This event resulted in an improvement of the nanocomposite's potential to store elastic energy and dampening ability. The dynamic storage modulus of the ND@GNP composites increased to 5.6 GPa, which was a ~143.5% increment over the neat EP. Furthermore, the glass transition temperature ( $T_g$ ) of the hybrid nanocomposites also increased with the filler loading, indicating the thermal stability of the composites.

The study conducted by Ribeiro *et al.* [109] was another example of the effectiveness of a hybrid nanofiller to induce superior thermal conductivity. In this study, they employed the hybrid of hexagonal boron nitride (h-BN) and GO in the polyurethane (PU) nanocomposite. The presence of h-BN assisted in better exfoliation of GO nanosheets and resulted in an increase in the nanosheets' specific surface area for better interfacial contact with the PU matrix. Additionally, the GO nanosheets also possess strong oxygen functional groups on their surface that also contributed to an enhanced interaction with the matrix. This led to a considerable amplification in heat transfer from the matrix to the conductive filler. On the other hand, the interaction between the hybrid fillers resulted in the formation of 2D structural units that provided a pathway for better phonon propagation.

The hybrid PU nanocomposite recorded an improvement of ~1,450% (1.7 W/m K) of thermal conductivity over the neat PU nanocomposites. Furthermore, consistent with the previously reviewed study, the improved fillers dispersion and interfacial interaction with the host polymer also resulted in significant augmentation of the mechanical properties of the composites. The tensile strength and Young's modulus of the hybrid PU composites improved by 85 (98 MPa) and 140% (73 MPa) compared to the neat PU.

Despite the applicability of hybrids in delivering good filler dispersion and unique nanofiller reinforcement structure in the composites, the ratio of the hybrid is still one of the crucial elements to be considered in

determining the synergy of the hybrids. Particularly, considering the variation in their types, dimensions, and sizes, the ratio of the hybrids can significantly affect the interaction and compatibility of the hybrid fillers which ultimately influence the thermal conductivity performance of the hybrid and the end properties of the nanocomposites.

Zhang *et al.* [74] investigated four different ratios of the hybrids RGO and AgNWs (RGO:AgNWs, 1:1, 1:2, 1:3, and 1:4) in EP nanocomposites. They found that at low AgNW content (1:1), RGO sheets were not fully exfoliated due to the low number of AgNWs. Meanwhile, at higher AgNW content (1:3 and 1:4), RGO sheets were insufficient to cover the nanowires which resulted in holes and also agglomerations. However, at the ratio of 1:2, the contents of RGO and AgNWs were appropriate to produce the synergy between the two fillers where RGO sheets could be completely inserted into the gaps of Ag nanowires. Additionally, the presence of AgNWs also prevented the graphene sheets from restacking and produced well-exfoliated RGO sheets. Thus, it can be simplified that the RGO sheets bridged the gaps between the silver wires; meanwhile, Ag wires linked the RGO sheets and prevented their  $\pi$ - $\pi$  stacking, establishing a succeeding 3D hybrid conductive network (Figure 4).

Besides the filler's ratios, the contents of the fillers also play a major function in determining the reinforcement performance of the hybrid fillers. Even at an appropriate hybrid ratio, low content of the hybrid can result in inadequate reinforcement, while, at high content of the hybrid, agglomerations still can occur which can be detrimental to the properties of the nanocomposites. Regarding thermal conductivity, a successive 3D nanofiller phonon conductive pathway must be built to ensure systematic phonon propagation. Hence, appropriate filler content must be used to form this unbroken filler network.

In this study, they showed that at a 1:2 RGO@AgNWs ratio, the best results of thermal and electrical conductivity were produced at 0.6 wt% of filler content. Owing to the good dispersion of the hybrid fillers, a consecutive 3D conductive structure could be achieved at the content of a low filler. On the other hand, increasing the content resulted in unused nanofillers which led to the fillers'



agglomerations. The hybrid RGO@AgNWs EP nanocomposite recorded a 66.7% improvement in the thermal conductivity ( $0.30 \text{ W/m K}$ ) over the neat EP and reduced the electrical resistivity of the composites by  $\sim 9$  orders of magnitude ( $4.8 \times 10^8 \Omega$ ). The storage modulus and  $T_g$  of the composites also increased up to 15.3% (2,831 MPa) and 4% (126°C), respectively, due to the physical confinement effect of the hybrid nanostructure in the matrix.

In some applications such as TIMs and electronic packaging, the materials need to have an outstanding thermal conductivity while also having an excellent insulating property [48,71,110–114]. Nanofillers like carbonaceous fillers, metals, and ceramic fillers often are thermally and also electrically conductive [47,59,71,111,115]. Hence, certain measures must be considered while engineering these materials to achieve the required properties.

One of the methods that can be employed is by hybridizing a thermally conductive filler with an electrically insulative filler such as h-BN and MoS<sub>2</sub>. However, this can lead to a considerable reduction in thermal conductivity since electrically insulative fillers might also have low thermal conductive properties. Nevertheless, the nanocomposites' thermal conductivity can still be preserved providing that the hybrid system has good dispersion in the host polymer.

For instance, Zhang *et al.*, [71] utilized ND with h-BN in EP nanocomposites. ND possesses a superior intrinsic thermal conductivity of  $2,000 \text{ W/m K}$  and can induce great conductivity properties in the insulative EP matrix. h-BN, on the other hand, only possesses  $125 \text{ W/m K}$  thermal conductivity. However, their study reported a paramount increase of 210% ( $0.54 \text{ W/m K}$ ) over the neat EP, which was 70% higher than the conductivity of the nanocomposites loaded with only h-BN at a similar concentration (29 wt%).

This outstanding increment was due to the good dispersion of the hybrid structure owing to their synergistic interaction. The attached ND on the h-BN surfaces hindered the agglomeration of the nanosheets and built an efficient 3D conductive network. The high conductivity of ND led to superior dissipation of heat flow; meanwhile, the homogenous distribution of h-BN helped to accelerate the heat propagation further, resulting in excellent thermal conductivity of the composite.

Furthermore, the uniform distribution of the hybrid fillers increased the interfacial adhesion of the nanofiller network with the matrix. This provided a sufficient interfacial contact between ND with the matrix to lend a crack pinning role when the polymer was subjected to an external force, resulting in augmented mechanical properties of the nanocomposite. The storage modulus of the

hybrid ND/h-BN EP nanocomposite increased up to 65% (3700.21 MPa), while the  $T_g$  increased from 115.94–167.07°C, respectively, due to the restriction of polymer chain mobility by the hybrid 3D network.

Interestingly, in a study conducted by Ribeiro *et al.* [48], they reported a considerable enhancement of 752% in thermal conductivity ( $1.02 \text{ W/m K}$ ) of PU nanocomposites when only h-BN was used as nanofiller to induce the thermal conductivity in the nanocomposite, and MoS<sub>2</sub> was utilized together as lubricative nanofiller to facilitate a homogenous distribution of h-BN. Though it was established that the thermal conductivity of h-BN is not as high as other nanofillers such as graphene, ND, AgNWs, *etc.*, it can be presumed that a moderate conductive filler can still result in outstanding conductivity when homogeneously dispersed.

Mechanical properties of the hybrid nanocomposites were also significantly improved due to the good dispersion of the hybrid filler which led to appropriate interfacial interaction between the filler network and the matrix. The crosslinking density, storage modulus, and failure strain at break, improved by 102, 106, and 10% over the neat PU ( $0.0061 \text{ mol/cm}^3$ , 13.89 Pa, 304%), respectively. Correspondingly, the brittleness of the hybrid composites was also reduced by 60% compared to the pure PU (0.025 Pa).

Meanwhile, in another study, they described a “zig-zag” effect of the combination of thermally conductive filler with electrically insulative filler to produce a hybrid system with thermal conductivity and electrical insulating properties. In this study, Wu *et al.* [59] used the hybrid of Ag nanoparticles with BN in EP nanocomposites. The insulative properties of BN served as insulation blocks that restricted the formation of conductive channels by Ag nanoparticles. The hybrid Ag/BN EP nanocomposites maintained their insulation properties within the range of insulating materials ( $10^{-12}$ – $10^{-15} \text{ S/cm}$ ), with low permittivity ( $\sim 4.7$ – $5.5$ ) and dielectric loss ( $< 0.2$ ).

Simultaneously, the thermal conductivity of the hybrid composites increased considerably from the synergistic effect of Ag nanoparticles and BN. The nanoparticles were grown on the surface of BN sheets and facilitated the restacking of the nanosheets to produce a hybrid network with uniform dispersion. In terms of thermal pathway structure, BN nanosheets acted as the leading passage for phonon transfers. On the other hand, the Ag nanoparticles on the surface of the nanosheets filled the gaps of the nanosheets and served as the “thermal bridges” for the inter-filler thermal network. This inter-filler network lowered the contact resistance during the phonon transfer for better thermal conductivity. Hence, the substantial increase

in the thermal conductivity of the hybrid composites achieved an increment of 1,089% (2.14 W/m K).

Similarly, in a study conducted by Yang *et al.* [11], the presence of SiO<sub>2</sub> in the hybrid also contained Ag nanowires and GNPs (AgNWs@SiO<sub>2</sub>&GNPs) in EP nanocomposite served as insulation links to break the electrically conductive channels of GNPs and AgNWs to retain the insulation properties of the composites. The interaction between graphene and silver could lead to a considerably high electrical conductivity; however, the coating of silica on the surface of AgNWs blocked the direct contact between the nanowires and nanosheets, hence hindering the electron transfer of this network, producing a hybrid nanocomposite material with low electrical conductivity of  $1 \times 10^{-5}$  S/cm.

The thermal conductivity on the other hand intensified greatly by the synergistic effect of these three nanofillers. The coating of SiO<sub>2</sub> onto the surface of AgNWs promoted a better dispersion of the nanofillers. Additionally, the presence of oxygenic groups on SiO<sub>2</sub> led to a decrease in the interfacial energy and an enhanced interaction with the host polymer. These also resulted in the better interconnection of GNPs with AgNWs@SiO<sub>2</sub> due to similar surface energy and the interaction of oxygenic groups on both surfaces. GNPs bridged the networks of AgNWs@SiO<sub>2</sub> by forming short and stiff covalent bonds between the silicone hydroxyl groups on the surface of AgNWs and the oxygenic groups on the plane surface of GNPs to produce an interminable conductive network. The thermal conductivity of the hybrid composites increased by 474% (1.0902 W/m K) from the neat EP, with a low electrical conductivity of  $1 \times 10^{-5}$  S/cm.

All of the discussed studies have greatly demonstrated the significance of employing hybrid nanofillers to produce better thermal conductivity properties of the thermoset composites. Moreover, the synergistic interaction of the hybrids also augments other aspects of the attributes of the nanocomposites including their mechanical properties which are very important considering the prospective applications of these nanocomposites.

To summarize the understandings gathered from the reviewed studies, it thus concluded that the key principle that produced the immense increment in the thermal conductivity in the hybrid nanocomposites was the improved dispersion of the nanofillers. A homogenous dispersion of these fillers increased their specific surface area and provided them with ample interfacial contact area with the host matrix for better heat dissipation, stress transfer, crack pinning, *etc.* Second, the compatibility of the hybrid fillers at an appropriate ratio and content also resulted in superior interaction of the fillers that built the 2D and 3D

continuous conductive network that was not only important for the heat transfer but also to reinforce the polymer with mechanical strength.

Also, the studies have established that using a moderate conductive filler could still result in satisfactory thermal conductivity due to the homogenous dispersion of the hybrid fillers. This allows the designing of hybrid systems with thermal conductivity and electrical insulative properties which can be very important in thermal interface materials such as electronic packaging.

Nonetheless, despite the encouraging results, further studies should still be carried out to further understand the hybrid synergy for better reinforcement application. Studies should also explore more the nanofiller dispersion method and nanocomposite preparation besides the filler ratio and content. Table 5 summarizes the properties of the nanocomposite for thermal management applications. From these published studies, it can be gathered that certain properties desired for these applications could be tailored by hybridizing different types of nanofillers of different characteristics. By selecting suitable nanofillers hybrid, and ranging their content and ratio, the characteristics required can be tuned to adjust to their needs.

## 6 Hybrid nanofiller in the barrier and tribological application performance

Diverse environmental and harsh working conditions expose steel surfaces and metal substrates to the permeation of aggressive species which can speed the process of metal corrosion. Hence, polymer coating and laminate films are designed as barriers to protect these substrates and ensure their durability. However, neat polymers such as EP often has low wear and chemical resistance due to their inferior mechanical strength such as low surface fraction energy and high brittleness [34].

Nanofillers such as metal oxides, NC, inorganic nanoparticles, and carbon-based nanomaterials are often incorporated into polymers to increase their mechanical, chemical, and tribological properties. These are due to their high chemical resistance and stability, excellent thermal property, outstanding tribological performance, low shear strength, high surface adhesion, *etc.* [34–38]. Graphene, for instance, possesses lower surface energy and can increase the composite's hydrophobicity [35]. The inclusion of these nanofillers provides the polymer with a physical barrier that improves the mechanical and wear performance of the composites (Figure 12).

Table 5: Hybrid nanocomposite properties for thermal management applications

| Matrix | Hybrid                      | Applications                      | Thermal conductivity (W/m K) | Volume resistivity ( $\Omega$ cm)         | Conductivity (S/cm)      | Storage modulus (GPa) | Tensile strength (MPa) | $T_g$ ( $^{\circ}$ C) | Reference |
|--------|-----------------------------|-----------------------------------|------------------------------|---|--------------------------|-----------------------|------------------------|-----------------------|-----------|
| EP     | GNP/ND                      | Electronic packaging              | 0.6–2.48                     | Not stated                                | Not stated               | 2.9–5.6               | Not stated             | ~112                  | [47]      |
| EP     | RGO/AgNWs                   | Antistatic and thermal conductive | 0.22–0.30                    | $2.2 \times 10^{10}$ to $4.8 \times 10^8$ | Not stated               | 2.8–2.3               | Not stated             | 126                   | [74]      |
| PU     | GO/h-BN                     | General                           | 0.6–1.7                      | Not stated                                | Not stated               | ~3.4                  | 80–98                  | Not stated            | [109]     |
| EP     | ND/h-BN                     | General                           | 0.23–0.54                    | Not stated                                | Not stated               | 2.4–3.7               | Not stated             | 167.07                | [71]      |
| PU     | MoS <sub>2</sub> /h-BN      | General                           | 0.5–1.02                     | Not stated                                | Not stated               | 2.5–2.9               | 52–60                  | Not stated            | [48]      |
| EP     | BN/Ag                       | Insulating materials              | 2.14                         | Not stated                                | $10^{-12}$ to $10^{-15}$ | Not stated            | Not stated             | Not stated            | [59]      |
| EP     | AgNWs@SiO <sub>2</sub> /GNP | Electronic packaging              | 0.25–1.09                    | Not stated                                | $1 \times 10^{-5}$       | Not stated            | Not stated             | Not stated            | [11]      |

Nonetheless, homogenous fillers distribution in the polymer matrix must be attained to accomplish a functional barrier with an extended diffusion protection path from the external environment. Besides, the nanofillers must also be incorporated in large doses to provide adequate protection. The problem that usually arises with large nanofiller contents is nanofiller agglomerations. Thus, incorporating hybrid nanofillers is one of the effective methods to provide a homogenous nanofillers distribution for enhanced nanocomposite properties.

The synergetic interaction between different fillers at working content and ratio can construct a well 2D/3D network barrier with sufficient defense properties even at lower dosages. The combination of appropriate nanofillers of complementing properties on the other hand can result in the reduction or elimination of undesirable properties, *i.e.*, high electrical conductivity can promote galvanic corrosion on defects on a long-time scale.

Additionally, nanofillers can also undergo surface modification to adopt new functionalities to the fillers such as hydrophobicity. A hydrophobic surface endows the coating with stronger impermeability characteristics to delay the substrate corrosion. Wu *et al.* [35] subjected RGO to different levels of fluorinated graphene oxide (FrGO) (low, moderate, and high) and found that graphene with the highest level of fluorine exhibited stronger inhibition properties initially. Nevertheless, the increase in RGO hydrophobicity made it difficult to achieve a homogenous filler dispersion. Thus, after 30 days of immersion, the RGO with lower levels of fluorination produced a better anti-corrosion performance.

They then hybridized FrGO with CeO<sub>2</sub> to improve the dispersion of the nanofillers. The decoration of CeO<sub>2</sub> on the surface of FrGO facilitated the dispersion of graphene nanosheets and increased the specific surface area of the hybrid networks for better interaction with the EP matrix. The uniform hybrid nanofillers distribution promoted the formation of a denser barrier network that can fill the micropores on the EP surface, increasing the impenetrability property of the composites for better corrosion performance. Moreover, CeO<sub>2</sub> possesses a cathodic inhibitor behavior that could absorb the surface of the steel and form a kind of passive layer to further block the penetration of the corrosive molecules (Figure 12).

It is also worth noting that the decoration of CeO<sub>2</sub> on the nanosheets' surface depended on the level of the RGO fluorination. The high content of fluorine caused a lowering in the surface energy and reduction in the active sites for the insertion of CeO<sub>2</sub>. Hence, the best anti-corrosion performance was produced by the hybrid of low FrGO and CeO<sub>2</sub> EP nanocomposite due to the optimal anticorrosion collaborative effect and synergy of the hybrid fillers.

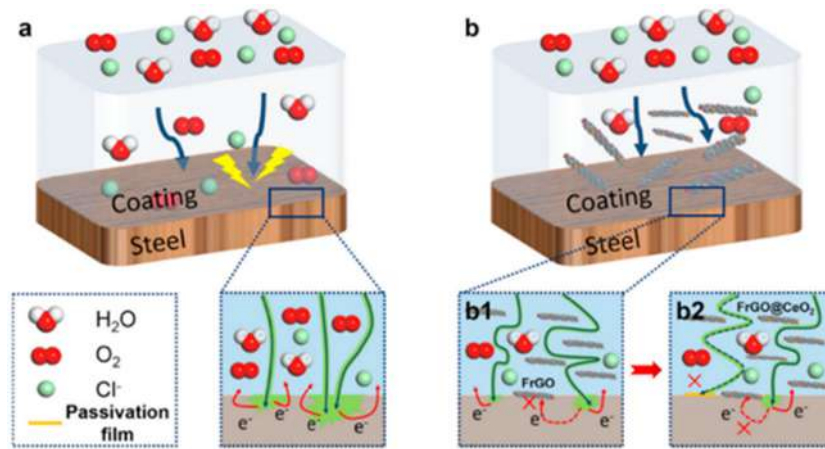


**Figure 12:** Schematic of nanofiller physical barrier mechanism to prevent the permeation of corrosive agents [35]. (a) pure waterborne epoxy coating, (b) composite coatings - (b1)FrGO; (b2) FrGO@CeO<sub>2</sub>.

After 30 days of electrolyte immersion, the impedance modulus ( $|Z|_{0.01\text{Hz}}$ ) of the hybrid coatings is still preserved at  $10^8 \Omega \text{ cm}^2$ , and charge transfer resistance ( $R_{ct}$ ) is maintained at  $2.44 \times 10^8 \Omega \text{ cm}^2$ , indicating remarkable corrosion resistance of the composites.

In another study [60], the incorporation of insulative filler in a hybrid system could endow the nanocomposite with self-healing properties. Ye *et al.* hybridized graphene and tetraaniline (TA) grafted POSS (POSS-TA) to reinforce the barrier properties of EP nanocomposite coating. TA possesses a good electroactivity and hybridizing it with graphene produced a hybrid system that endowed the nanocomposite with well-insulating and self-healing properties. The modification of POSS-TA onto the graphene layers improved the dispersion of graphene, which resulted in a continuously impenetrable barrier for better inhibition of the diffusion of aggressive molecules. Simultaneously, POSS-TA layers were also evenly distributed on the graphene layers, forming a highly interactive resistance network.

During a shielding effect, the hybrid protective layer would block the penetration of corrosive particles. Concurrently, the electroactive POSS-TA would bind the present electrons and change them from a reduced state to an intermediate oxidation state. Meanwhile, the oxygen would oxidize the iron ions to ferrous oxide and iron oxide and build a passive layer on the substrate. Additionally, the reduced POSS-TA could also be oxidized onto the intermediate oxidation state and released two electrons which further promoted the generation of the passive layer. The rebound values of  $|Z|_{0.01\text{Hz}}$  ( $2.13 \times 10^9$  to  $2.76 \times 10^9 \Omega \text{ cm}^2$ ) were recorded for the hybrid nanocomposite coating with immersion from 80–100 days which indicated the efficiency of the hybrid for self-healing ability.

Other than the corrosion resistance properties, the friction and wear rate of the composite materials are also the major factors to guarantee the integrity of their protective performance. A nanocomposite material with good mechanical properties can endure stress under friction and does not wear easily which makes it extremely practical for long-term uses. Nanofiller such as graphene are often used owing to their high intrinsic mechanical properties. Nevertheless, it has been constantly reported that graphene platelets agglomerate at high filler loadings. Furthermore, due to the hardness of the surfaces, high contact forces, and accumulation of heat flux can occur during the sliding/rolling which can be damaging to the material.

Hybridizing graphene with softer material such as MoS<sub>2</sub> can provide lubrication to the hybrid system and produce an easier rubbing process. In a study conducted by Upadhyay and Kumar [36] employing this hybrid for EP nanocomposite, they recounted that in this hybrid system, graphene nanosheets were situated aligned to the sliding direction, while MoS<sub>2</sub> was interspersed between the graphene sheets. During sliding, due to the low adhesion bonding between the layers, the nanofillers on the top surfaces detached and filled the vacant surfaces of the composites, forming a tribo-layer film to minimize the adhesion forces (Figure 13). In addition, the presence of graphene also restricted the interaction of MoS<sub>2</sub> with the external surrounding at high humidity (Figure 14). MoS<sub>2</sub> undergoes oxidation when the water content is high which could significantly reduce its lubrication ability.

Furthermore, the significance of the hybrid ratio and content to ensure the effectiveness of the hybrid performance were also discussed in this study. First, the hybrid nanofillers were combined at an equal ratio (50:50) due to their different

properties. Adding a higher ratio of graphene could cause unnecessary high brittleness to the composites due to the hardness of the nanofiller. On the other hand, adding a higher ratio of  $\text{MoS}_2$  could induce the cumulation of harmful oxides. When an equivalent portion was used, these opposite characteristics could balance each other to produce a coactive and synergistic effect for more efficient performance. Thus, under different humidity levels, loads, and sliding cycles, the hybrid composites retained a low coefficient of friction (COF) and wear rate ranging between 0.0019 and 0.01 and  $1.0$  and  $1.48 \times 10^{-7} \text{ mm}^3/\text{Nm}$ , respectively.

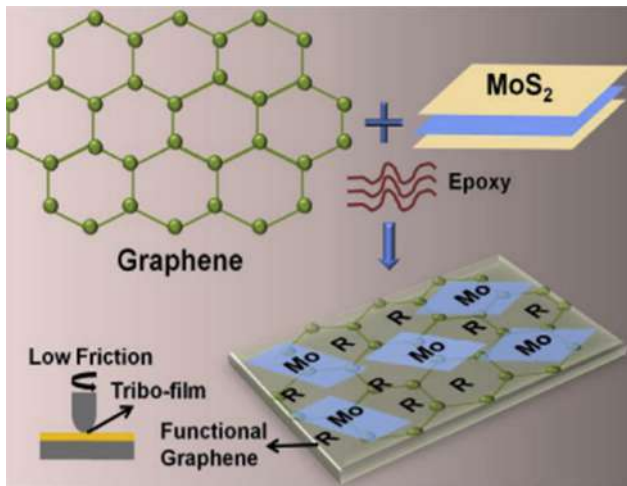


**Figure 13:** Illustrative diagram and system of functional graphene in the structure of tribo-film on the surface of ternary composites [36].

Another study carried out by Chen *et al.* [33] also employed the use of hard nanofillers (CNT and GO) and soft nanofillers ( $\text{MoS}_2$ ). Similarly, they found out that the use of this type of hybrid system was very effective to enhance the friction and wear properties of the polymer nanocomposites. CNT and GO possess very high mechanical strength and provided robust stress transfer properties of loading during sliding and friction. Meanwhile,  $\text{MoS}_2$  with its self-lubricating effect minimized the friction and allowed the process to run smoother. Additionally, the presence of each nanofiller helped to uniformly disperse the nanofillers inside the EP matrix, thus adding to the synergistic effect of these fillers.

During the friction and wear process, the hybrid EP-CNTs/GO/ $\text{MoS}_2$  nanocomposite produced smaller debris compared to neat EP, EP-CNTs/GO, and EP-CNTs/ $\text{MoS}_2$  nanocomposites due to the improved tribological performance. This debris could be transformed onto transfer films and lodged into the grooves of the worn surfaces and protected the composites from direct contact with the steel ball, reducing the friction force and enhancing the wear resistance (Figure 15). The COF and wear rate of the hybrid composites were reduced by 90 (0.042) and 95% ( $3.44 \times 10^{-5} \text{ mm}^3/\text{Nm}$ ), respectively, compared to the pure EP.

Additionally, the thermal properties of the EP-CNTs/GO/ $\text{MoS}_2$  nanocomposite indicated satisfactory thermally stable properties. Its thermal decomposition temperature at 5% mass loss was  $304.2^\circ\text{C}$ , which was 12.9% higher than the neat EP. Meanwhile, its residual weight fraction

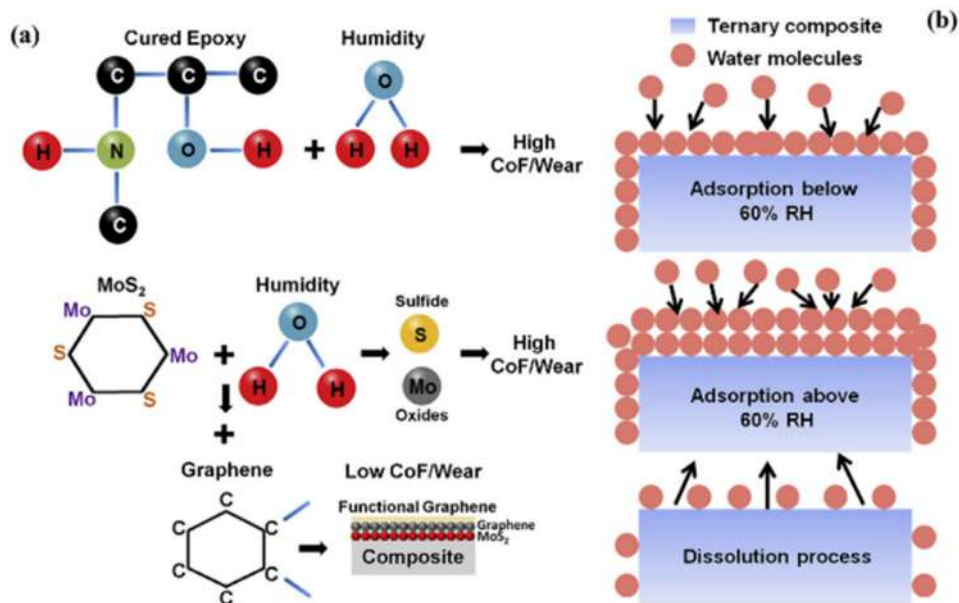


**Figure 14:** (a) Wear mechanism of EP,  $\text{MoS}_2$ /EP composites, and graphene/ $\text{MoS}_2$ /EP composites and (b) adsorption system of water molecules on the composite surfaces under distinct humidity environments [36].

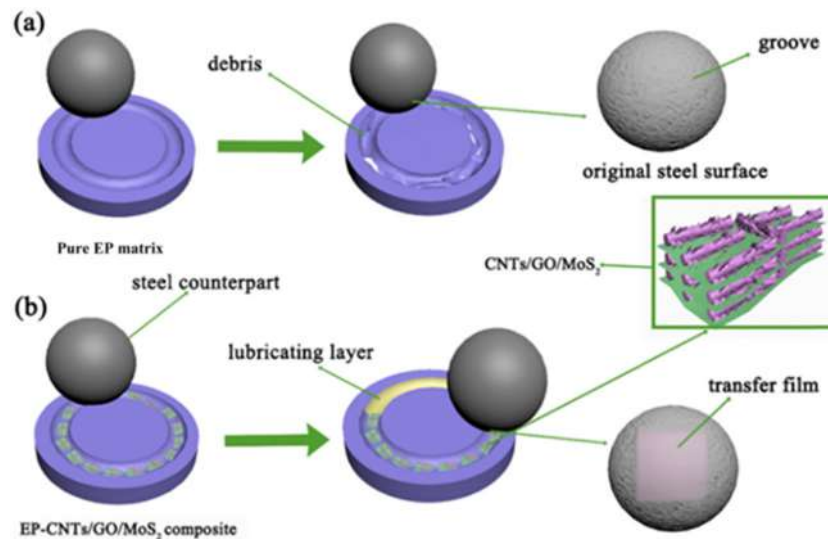


**Figure 15:** The mechanism of hybrid nanofillers lubricating layer to transform to transfer films [33]. (a) pure EP; (b) EP-CNTs/GO/MoS<sub>2</sub>.

at 500°C retained a value of 16.8 wt%, which was considerably bigger than the neat EP (3.8 wt%). These significant improvements were due to the good dispersion of the hybrid system, which acted as a physical barrier that prevented the transfer of the decomposed products out of the nanocomposite. During a friction and wear process, heat is generated that can soften the composite material. Thus, having thermally stable properties can ensure the durability of the nanocomposite.

Another excellent tribo-layer performance of hybrid nanofillers interaction was reported by Yan *et al.* [34]. Herein the hybrid of titanium carbide (Ti<sub>3</sub>C<sub>2</sub>) and graphene was used to construct wrapping nanofiller structure by bridging the effect of polydopamine (PDA) (Figure 16) to enhance the tribological properties of EP coating. The upper layer of graphene acted as the primary barrier and lubrication network, while the second layer of Ti<sub>3</sub>C<sub>2</sub> functioned as the supplementary layer that provided further defense and auxiliary support after graphene is expended. This multi-layered structure is performed as compensating lubrication system to prevent rapid consumption of lubricant and guarantee a durable and long-lasting performance of the coating. The COF and wear rate of the hybrid composites significantly decreased by ~11 (0.50) and ~88% ( $1.18 \times 10^{-4} \text{ mm}^3/\text{Nm}$ ) compared to pure EP.  $|Z|_{0.01\text{Hz}}$  of the hybrid after friction decreased only by 11.01% ( $1.90 \times 10^9 \Omega \text{ cm}^2$ ) compared to the initial  $|Z|_{0.01\text{Hz}}$ , which was ~8 times lower than the reduction in the pure EP, indicating the upheld integrity of the hybrid and the sturdiness of the wrapping structure to shorten the composites diffusion path.

Table 6 summarizes the properties of the nanocomposite for application in barrier protection. In summary, the diverging characteristics of different nanofiller types play significant roles to produce complementary effects which work collaboratively to yield high-performance tribological properties of polymer composites. Many forms of hybrids can be designed to explore their interactions

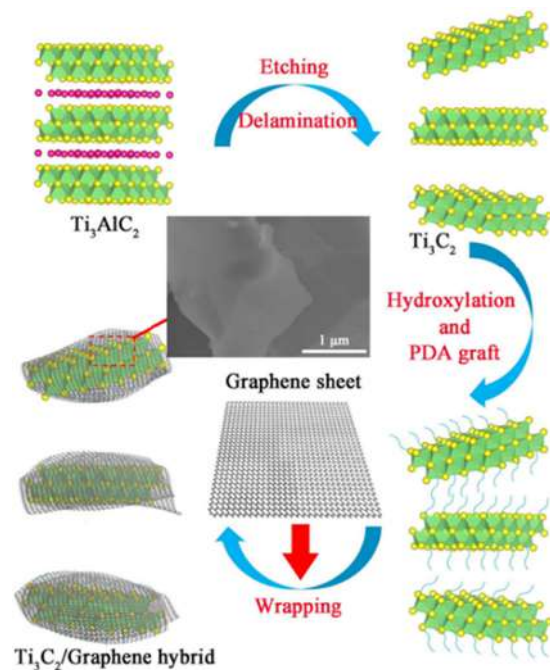


**Figure 16:** The graphic diagram of the assembly method of the wrapping structure of Ti<sub>3</sub>C<sub>2</sub>/graphene hybrid [34].

Table 6: Hybrid nanocomposite properties for barrier and tribological applications

| Matrix | Hybrid                            | Application                   | COF         | Wear rate<br>(mm <sup>3</sup> /Nm) | Impedance<br>modulus<br>( Z  <sub>0.01Hz</sub> ) (Ω cm <sup>2</sup> ) | Coating<br>resistance<br>(R <sub>c</sub> ) (Ω cm <sup>2</sup> ) | Charge transfer<br>resistance<br>(R <sub>ct</sub> ) (Ω cm <sup>2</sup> ) | Water<br>uptake<br>(vol%) | Oxygen permeability<br>coefficient (cm <sup>3</sup> cm/<br>cm <sup>2</sup> s Pa) | Reference |
|--------|-----------------------------------|-------------------------------|-------------|------------------------------------|---|---|--|---------------------------|--|-----------|
| EP     | FG/CeO <sub>2</sub>               | Coating                       | Not stated  | Not stated                         | ~10 <sup>8</sup> (30 days<br>immersion)                               | ~10 <sup>7</sup> (30 days<br>immersion)                         | ~10 <sup>8</sup> (30 days<br>immersion)                                  | Not stated                | Not stated   | [35]      |
| EP     | POSS-TA-G                         | Coating                       | Not stated  | Not stated                         | ~10 <sup>9</sup> (100 days<br>immersion)                              | Not stated  | Not stated   | 3.8                       | 1.45 × 10 <sup>-14</sup>   | [60]      |
| EP     | G/MoS <sub>2</sub>                | Rolling/sliding<br>components | 0.0019–0.01 | 1.0–1.48<br>× 10 <sup>-7</sup>     | Not stated  | Not stated  | Not stated   | Not stated                | Not stated   | [36]      |
| EP     | Ti <sub>3</sub> C <sub>2</sub> /G | Coating                       | 0.50        | 1.18 × 10 <sup>-4</sup>            | 1.90 × 10 <sup>9</sup> (after<br>friction)                            | Not stated  | Not stated   | Not stated                | Not stated   | [34]      |
| EP     | CNTs/GO/MoS <sub>2</sub>          | Coating                       | 0.042       | 3.44 × 10 <sup>-5</sup>            | Not stated  | Not stated  | Not stated   | Not stated                | Not stated   | [33]      |

and properties to tune them to the performance needed for the applications.

## 7 Hybrid nanofiller in hydrogen storage materials

Hydrogen possesses large chemical energy (~143 MJ/kg), which was about three times greater than the energy density of petroleum and thus, has been considered the leading-edge energy carrier in the applications such as mobile and stationary power sources [61,63,116]. Its broad availability and non-toxicity make it a fitting prospect for feasible clean energy sources and green technology that can substitute the consumption of non-renewable fossil fuels [61].

The storage of hydrogen gas can be either through chemisorption in hydrides or physisorption in porous materials with high surface areas [61,63]. Moderate sorption and desorption temperature, swift kinetic and volumetric hydrogen mass, as well as satisfactory reversibility, are among the qualities needed for this application [62,117]. Nanoparticles from carbon-based materials, metal hydrides, and transition metals have been studied on their capacity to bind and store hydrogen gas [61,62]. Oftentimes, these particles are confined in polymer matrices, e.g., PANI and polyetherimide (PEI) which act as a selective barrier that regulates the sorption and desorption cycles by these fillers [61,63,118]. However, regardless of the potential held by these hybrid nanocomposites, the studies utilizing their effects are still scarce.

Carbon-based materials such as graphene sheets are one of the materials that can be incorporated into the polymer matrix to facilitate hydrogen binding and retention [61,119]. However, at ambient temperatures, the binding energy between graphene sheets and hydrogen weakens which causes a lowering in the storage capacity of this nanofiller [61,119]. Chemical and structural modifications are one of the approaches that can be implemented to address this drawback. One of the instances is the decoration of transition metals such as palladium (Pd), platinum (Pt), and titanium (Ti) on the surface of graphene [61,120]. These metals possess high hydrogen adsorption efficacy and also a high catalytic activity that can act as catalysts for hydrogen conversion. The combination of these metals with carbon-based nanofillers can lead to a synergistic performance to further enhance the hydrogen storage of the hybrid fillers [61,120].

Nevertheless, direct doping of these metals on the carbonaceous nanofillers has been reported to cause

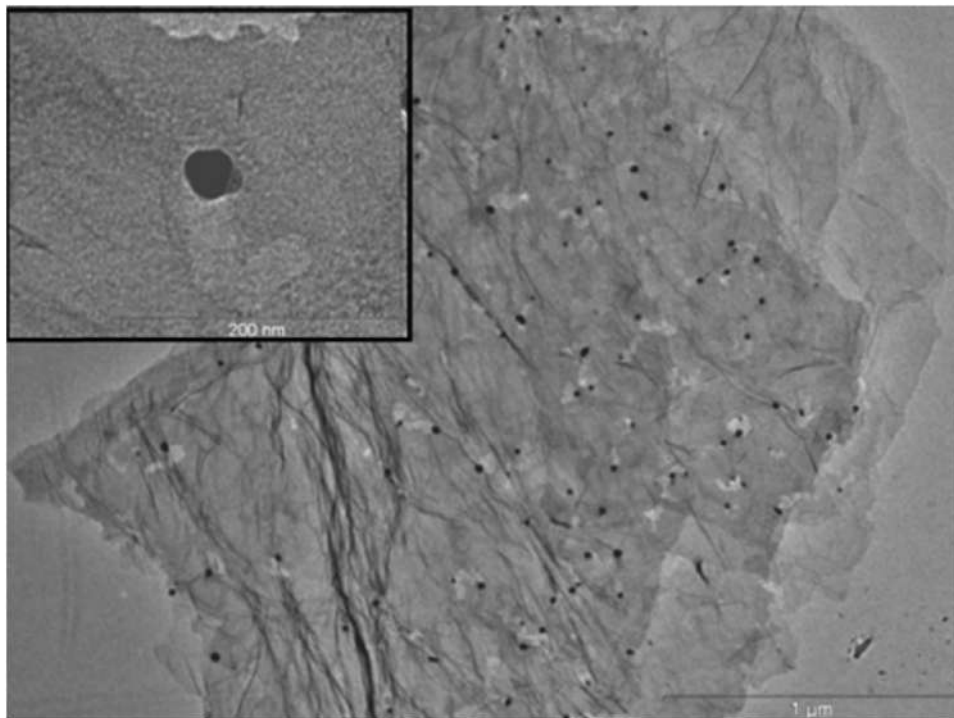


**Figure 17:** TEM micrograph of RGO nanocomposite. The bright particles are Pd and the darker particles are Al<sub>2</sub>O<sub>3</sub> [61].

agglomerations which lowered the amount of the active sites for hydrogen adsorption [61]. Thus, a supporting material must also be incorporated to assist the dispersion of these metals to establish the synergistic effect between the hybrid metal and the carbonaceous filler for improved hydrogen storage capacities.

In a study by Bajestani, Yurum, and Yurum [61], Al<sub>2</sub>O<sub>3</sub> was employed to facilitate the dispersion of Pd. First, the hybrid of Al<sub>2</sub>O<sub>3</sub>/Pd was synthesized by adding palladium chloride into the dispersion of Al<sub>2</sub>O<sub>3</sub>. This hybrid was then added to the RGO solution to form Pd/Al<sub>2</sub>O<sub>3</sub>-decorated graphene sheets. The combination of the lower and higher energy of Pd, Al<sub>2</sub>O<sub>3</sub>, and oxygen in RGO led to the synergistic interaction between the hybrid structure that formed a homogenous filler distribution (Figure 17).

Furthermore, their results showed that the particle size of Al<sub>2</sub>O<sub>3</sub> also played a significant role in determining the synergy and efficiency of the hybrid. The smaller size of Al<sub>2</sub>O<sub>3</sub> led to a higher decrease in the Brunauer-Emmett-Teller surface area and total pore volume, indicating a better distribution of Pd/Al<sub>2</sub>O<sub>3</sub> hybrid on the spaces of graphene sheets. This led to an improvement of 82% of the hydrogen uptake (0.31 wt%) compared to the uptake presented by the pristine RGO (0.17 wt%). This improvement was also complemented by the increase in the slope of isotherms in the intermediate and high-pressure

regimes which showed the activation of a spillover process. In this process, the presence of the weak Lewis acid sites in the  $\gamma$ -Al<sub>2</sub>O<sub>3</sub> promoted the diffusion of hydrogen atoms on its surface, thus resulting in the enhancement of the hydrogen uptake of the hybrid nanocomposite.

In addition, metal hydrides are also among the particles of interest for the chemisorption of hydrogen gas due to their high gravimetric hydrogen density, adequate thermodynamics, low reactivity, and low storage pressure [62,121]. Sodium alanate (NaAlH<sub>4</sub>) for instance possesses a high gravimetric capacity, which theoretically can reach a hydrogen content of 7.4 wt% [62,122]. However, its high desorption temperature restricts its reversibility and applications [62,123]. The hybridization with carbon-based materials and transition metals has been found to effectively lower the reaction temperature, enhance the reaction kinetics, and ameliorate the reversibility [62].

Beatrice *et al.* [62] studied the hybrid NaAlH<sub>4</sub>/MWCNT system in sulfonated polyetherimide (PEIS) on the hydrogen storage activity of the hybrid nanocomposite. The use of MWCNT improved the thermal stability of the hybrid composite due to the intrinsic high stability of MWCNT. This is particularly important because it could protect the fillers from extensive exposure to oxygen and moisture as sodium alanate is significantly sensitive to them. Simultaneously, the presence of NaAlH<sub>4</sub> also improved the dispersion of MWCNT in the PEIS matrix by penetrating between the



nanotubes, detaching them, and preventing them from agglomerates. This increased the specific surface area of the hybrid nanostructure and increased the hydrogen storage kinetic. Furthermore, the intrinsic hollow structure of MWCNTs provides a facile route for the delivery of the hydrogen gas on the surface of  $\text{NaAlH}_4$ , leading to an escalated hydrogenation process. After 6 h, they observed an 80% increment in the hydrogen storage absorbed by the hybrid PEIS nanocomposites (0.9 wt%) compared to the nanocomposite containing only  $\text{NaAlH}_4$ .

Besides the hydrogen storage capacity, the reusability and the structural stability of these nanocomposites are also immensely essential, particularly when considering their efficiency for long-term applications. PEI is also known to possess outstanding chemical resistance, thermal stability, and mechanical properties. And the incorporation of hybrid nanofillers would boost these excellent features further, in addition to the increase in the hydrogen storage ability.

Muthu *et al.*, [63] studied the reusability of PEI membrane nanocomposite reinforced with halloysite nanotubes (HNTs) and BN. Their result showed that after five cycles of hydrogenation/dehydrogenation using the thermal annealing method, the hybrid membrane composite could still retain hydrogen storage up to 91.43%. Furthermore, the X-ray diffraction tests on the membrane also suggested that this membrane could heal itself after repeated cycles (5 cycles). These results increased the prospective potential of this nanocomposite for various fuel cell applications.

Furthermore, the synergistic effect of the hybridization between HNT and h-BN also led to a remarkable storage capacity. HNT possesses outstanding adsorption amplitude, high specific surface area, high porosity, and a long-life cycle. Meanwhile, the heteropolar band of B and N atoms in BN provides a surface with intense interaction with hydrogen molecules which may lead to enhanced absorption of hydrogen. The decoration of BN on HNT enhanced the dispersion of HNT and increased the interlayer spacing of the nanofillers which offered more storage of hydrogen. Additionally, the presence of BN also facilitated a higher absorption of hydrogen gas due to the dipolar nature of BN. Their study reported a hydrogen storage capacity of 4.2 wt% by the hybrid nanocomposite, which was 425% higher than the pure PEI, and 16.7 and 75% higher than the nanocomposites containing only HNT and BN.

These studies showed the effectiveness of incorporating hybrid nanofiller systems to improve the hydrogen storage performance of thermoset materials. First, the synergistic interaction between the fillers during hybrid preparation results in the homogenous nanofillers dispersion in the

matrix. This will then increase the specific surface area of the hybrid structures which is essential for efficient and enhanced hydrogen adsorption. Second, the synergistic interaction of the fillers also balances and augments the properties and mechanisms of the hybrid reinforcement, resulting in comprehensive hydrogen storage performance of the nanocomposite material. Furthermore, the hybrid network will also boost the mechanical properties of the composites which can ensure material stability for long-term applications.

## 8 Hybrid nanofiller in bio-thermoset polymer

The shortage of non-renewable resources and raised sensitiveness of eco-sustainability have shifted the manufacture of many polymers toward renewable resources to replace fossil fuels [64,98]. However, many reports showed that bio-based thermosetting polymers suffer a few drawbacks in the final properties which limit their widespread applications including high flammability, low glass transition temperature, low fracture toughness, poor elongation at break, and poor mechanical properties [64,124]. To overcome these shortcomings, several methods have been proposed, including the addition of various fillers such as graphene, ferrite, polyaniline nanofiber (PN), carbon dot (CD), *etc.* [64,98,124]. Nevertheless, the studies involving hybrid nanofiller reinforcement in bio-based thermosetting polymers to date are still scarce.

One of the most dominant factors that cause the unsatisfactory properties of bio-based polymers is due to the lowering of the crosslinking density [64,125]. This leads to a reduction in the glass transition temperature, thermal stability, mechanical properties, *etc.* Generally, nanofillers are incorporated into polymers as a physical reinforcement that can improve these properties by several mechanisms such as hindering the polymer chain motion and providing an interfacial contact for stress transfer from the matrix to the filler structure. However, the utilization of certain nanofillers can also increase the crosslinking density through the interactions of the functional groups in both the fillers and the matrix [64].

For instance, a study by Saikia *et al.* [64], using PN and CD (PC) as nanohybrid reinforcement in a bio-based EP (the blend of bisphenol-A, sorbitol, and monoglyceride of castor oil), found that the oxygenous groups present in the graphitic PC, as well as the nitrogen-containing polymeric backbone of PN, could interact with the

**Table 7:** Recent hybrid nanocomposite materials with their special characteristics and properties

| Hybrid material   | Special characteristic  | Properties  | Ref. |
|---|---|---|------|
| EP-based CFRPs laminate containing CNT/ GNP hybrid                    | Lightning strike protection and EM shielding                        | Electrically and thermally conductive   | [52] |
| PFB nanocomposites containing CNT/ AgNFs/CB hybrid                    | Degradable and fully recyclable for 3D-printed wearable electronics | <ul style="list-style-type: none"> <li>– Self-healing</li> <li>– Electrically conductive</li> <li>– Piezoresistive</li> <li>– Excellent mechanical performance</li> </ul>   | [54] |
| Porous EP composites reinforced with GO/ CNTs hybrid                  | Microwave absorber  | <ul style="list-style-type: none"> <li>– Reduced density</li> <li>– Electrically conductive</li> <li>– Improved absorption performance</li> <li>– High permittivity</li> <li>– Improved RL performance</li> </ul> | [56] |
| EP nanocomposite containing ND/h-BN hybrid                            | TIM   | <ul style="list-style-type: none"> <li>– Thermally conductive</li> <li>– Superior dissipation of heat flow</li> </ul>   | [71] |
| EP nanocomposite containing Ag/BN                                     | TIM   | <ul style="list-style-type: none"> <li>– Thermally conductive</li> <li>– Electrically insulative</li> </ul>   | [59] |
| EP nanocomposite containing POSS/TA hybrid                            | Protection layer  | <ul style="list-style-type: none"> <li>– Self-healing</li> <li>– Shielding effect</li> </ul>  | [60] |
| EP coating containing Ti <sub>3</sub> C <sub>2</sub> /graphene hybrid | Protective coating  | <ul style="list-style-type: none"> <li>– Enhanced tribological performance</li> <li>– Lubricating</li> <li>– Durable</li> </ul>   | [34] |
| PEIS containing hybrid NaAlH <sub>4</sub> /MWCNT                      | Hydrogen storage material   | <ul style="list-style-type: none"> <li>– Thermally stable</li> <li>– Improved hydrogen storage kinetic</li> </ul>   | [62] |
| Sulfonated polyetherimide membrane containing HNT/BN hybrid           | Hydrogen storage membrane   | <ul style="list-style-type: none"> <li>– Reusable</li> <li>– Remarkable hydrogen storage capacity</li> </ul>  | [63] |

polar functional groups of the bio-EP matrix. This secondary interaction increased the crosslinking density of the matrix and consequently improved the other properties of the hybrid biocomposites including their mechanical properties, thermal stability, and chemical resistance.

Furthermore, the presence of polar–polar interactions and hydrogen bonding between the hybrid fillers led to a good filler dispersion in the host matrix. CD possesses a great number of functionalities and could alter the surface of PN to facilitate its dispersion. This resulted in the synergistic effect of the formation of a homogenous nanofillers distribution with a high aspect ratio and maximized use of the surface functionalities for a stronger interaction with the matrix. Moreover, during a mechanical test, the graphitic layers of CD provided a sliding effect, while, the aromatic aniline moieties of PN offered a stronger backbone with the aromatic chain. This led to a significant enhancement in the elongation and flexibility of the bio nanocomposites.

Additionally, the corrosion protection mechanisms of the bio nanocomposites are also considerably improved

by the reinforcement of the hybrid PC. The existence of the conductive moieties in PC inhibited the anodic and cathodic sites, hindering the corrosion in the saline medium. Besides, the homogenous dispersion of the hybrid nanofillers and the strong interaction between the fillers with the matrix also provided a robust barrier to the permeation of the corrosive molecules.

The tensile strength, elongation at break, scratch resistance, and impact resistance of the hybrid biocomposites recorded an improvement of 36.4 (30 MPa), 30.4 (45%), and 42.9 (>10 kg), and 77.1% (14.75 kJ/m<sup>2</sup>) compared to the neat polymer. Meanwhile, the endset degradation temperature of the composites increased by 11°C (482°C) with the char residue increasing by 69.2% (4.4% at 700°C). The nanofillers network also presented an excellent barrier performance with a corrosion rate of  $5.68 \times 10^{-3}$  mils per year.

In some cases, renewable resources such as vegetable oils are blended with polymer to provide plasticizing effects such as improving the polymer's toughness

[65], enhancing the interaction between the polymer and fillers [126], and easing the processing of the polymer [127]. However, due to the limited numbers of unsaturated bonds of these oils, the production of the epoxide functional groups is also restricted. This often leads to a reduction in the crosslinking density that can adversely affect the properties of the bio-blend material [128]. The incorporation of nanofillers, particularly the hybrid can ameliorate these problems and reinforce the bio nanocomposite.

Panda *et al.* [65] designed the partially biodegradable nanomaterial of unsaturated polyester (UPE)/epoxidized soybean oil acrylate (ESOA) blend composites with the reinforcement of chitosan (CS) functionalized GNP for multidisciplinary nanoengineering applications. The interaction between the carboxyl group of GNPs and amino groups of the CS formed amide bonding gave a structure to the CS wrapping the surface of GNPs and improved the dispersion of GNPs inside the matrix. The epoxide group of GNPs, the amino group of CS, and hydroxyl, carboxyl, and carbonyl moieties in the UPE/ESOA matrix interacted together to build a highly synergetic nanocomposite construction.

The properties of the hybrid composites improved dramatically compared to the composites containing only GNPs. The tensile strength, strain, Young's modulus, impact strength, and hardness increased by 67.9 (94 MPa), 5 (1.9%), 37.2 (5 barrier. 27 GPa), and 76.9 (115 J/m), and 67.3% (82 shore D). The storage modulus and  $T_g$  improved by ~36% (6,800 MPa) and 20°C (145°C), respectively, indicating the thermal stability of the hybrid. Thermal conductivity and dielectric strength improved by ~200 (0.9 W/m K) and ~7% (16.5 kV/mm) with volume and surface conductivity of  $6.5E \pm 10^{-5}$  and  $3.8E \pm 10^{-7}$  S/cm.

Besides strengthening the biothermoset polymers, the reinforcement of hybrid nanofillers can also result in special properties in the bio nanocomposites such as flame retardancy and microwave absorption ability. These types of features, combined with good mechanical, thermal, and other essential properties, can increase the biopolymer's potential to replace conventional polymers for future commercial-industrial applications.

Acuna *et al.* [124] developed biomass castor oil-based rigid polyurethane foam (RPUF) nanocomposites containing modified polyols from castor oil. The hybrid of expanded graphite (EG) and GO was incorporated to improve the composites' flame retardancy and high insulation capacity. The inherent morphology of EG is effective to halt the spread of the fire as it can expand and block the fire feeding during the combustion process. Meanwhile, GO on the other hand is effective as a barrier against oxygen penetration which can stop the further spreading of the fire.

Moreover, the addition of GO to EG endowed EG with better dispersion in the matrix and restricted the increase in thermal conduction in the solid state. Furthermore, the intrinsic properties of GO as a gas barrier also delayed the diffusion of gases and decreased heat transfer. Compared to the composites containing only EG, the thermal conductivity of the hybrid composites was significantly reduced by 10.5% (34.2 mW/m K) after the inclusion of GO. UL94 test of the hybrid also established a V-0 rating with a brief burning time of only 17.9 s. The heat release rate (HRR), total heat release (THR), and total smoke production (TSP) were also effectively reduced by 54 (178 kW/m<sup>2</sup>), 24 (17.3 MJ/m<sup>2</sup>), and 15% (6.0 m<sup>2</sup>).

Bikdeli *et al.* [98] conducted a study on the incorporation of a ternary hybrid of magnetic filler manganese ferrites ( $Mn_xFe_{3-x}O_4$ ), dielectric filler nickel oxide (NiO), and conductive filler PANI to introduce a high-performance microwave shielding ability to bio-based PU coating nanocomposites containing vegetable polyol based on epoxidized soybean oil and methylene diphenyl diisocyanate. The combination of magnetic and dielectric loss, as well as enhanced composite conductivity, amplified the effectiveness of the microwave absorption capacities.

Additionally,  $Mn_xFe_{3-x}O_4$  contributed to the main decline in the reflection from the surface of the composites (69.46%). However, the percentages of other fillers, combined with  $Mn_xFe_{3-x}O_4$  led to the synergetic effect that significantly enhanced the productivity of the microwave absorption performance. Thus, an optimum RL value less than -30 dB, equivalent to 99.9% of microwave absorption over the X-band frequency range (8–12 GHz) was achieved at the filler concentrations of 1.5 wt% of  $Mn_xFe_{3-x}O_4$  and NiO and 1 wt% of PANI.

Based on these published studies, it can be gathered that the incorporation of hybrid nanofillers into the biothermoset polymer can ameliorate the drawbacks of blending the conventional resin with biological resources. The increase in the crosslinking density for instance will result in better thermal stability and improved mechanical performance of the bio nanocomposite. On the other hand, other features can also be equipped into these biothermosets depending on the intrinsic properties of the hybrid nanofillers. This will encourage the prospect of further development and commercialization of biothermosets in various applications.

## 9 Challenges and future perspective

The incorporation of nanofillers as thermoset and biothermoset reinforcement has been established as one of the

most effective ways to equip polymers with the required properties of the demanded applications. Besides the nanofillers' diverse characteristics, their easy accessibility and renewability, as well as the lightweightness of the fillers make them a very attractive alternative to numerous other reinforcement particles. Various types of characteristics could be designed and implemented into the polymers by combining different types of fillers to produce the hybrid reinforcement desired by the polymers [129–133,134].

With the advance in technologies and demands of the prospective lifestyle, futuristic applications of revolutionary properties are essential. Nanofillers with their abundance and easy accessibility can be a facile access for modulating and conceiving these implementations. However, the fundamental science of nanofiller chemistry and reaction must be grasped comprehensively to apprehend the interaction of the hybrid fillers in the polymer matrix as well as their interactivity with the matrix itself. Comprehending this aspect on the cardinal level can help to broaden the innovation of nanocomposite applications further in the future.

The interaction of the hybrid nanofillers is particularly vital to be penetrated, specifically on the role of the ratio and concentration of the hybrid that promotes the synergistic effects. Many studies have shown heterogeneous results typically when inconsistent techniques and dispersion methods are used. This is of significant importance to comprehend particularly in the designing of large-scale fabrication of nanocomposite materials.

On the other hand, the processing and recovery of nanofillers should also be made easier to ensure the simple and feasible accessibility of these fillers. Studies should be carried out to maximize the synthesis of these fillers and the properties produced by the different types of synthesis and recovery methods. Meanwhile, a more effective procedure should also be explored to accommodate nanofillers in the polymer matrices that can intensify the interaction and compatibility between the nanofiller and the matrix. Also, an in-depth study of the stability of these nanofillers within the polymer matrix with time should be analyzed to assure the longevity of the nanocomposite's applications.

## 10 Conclusion

The research involving hybrid nanofiller systems has been growing tremendously in numerous sectors. Table 7 summarizes the recent materials comprised of hybrid nanofiller and their special characteristics and properties.

The abundance of extremely beneficial properties of nanofillers is very constructive to design a variety of tunable properties in ranging thermosets applications. Furthermore, many industries are progressing rapidly, thus substantially increasing the need for multifunctional and robust thermoset performance. The inclusion of nanofillers can improve the prevailing thermoset properties such as their mechanical, chemical, and conductivity, as well as introduce new properties such as lubricating systems and flame retardancy ability.

Hybridizing different nanofiller types have been vastly reported to result in better enhancement of composites' properties compared to the single nanofiller reinforcement systems. Generally, from the discussion of the previous works, it can be deduced that the incorporation of hybrid nanofillers reinforcement in thermoset and biothermoset composites are significantly promising to produce composites of durable and adaptable properties. Below are some of the conclusions that we can summarize from these published studies:

- At optimum hybrid ratios and concentrations, synergistic interaction between nanofillers can be expected, which will lead to a better filler dispersion inside the polymer matrix, increasing the aspect ratio of the hybrid system, and also improving the adhesion between the filler and the matrix. This ultimately results in the enhancement of the nanocomposites' properties such as the mechanical and thermal properties, and other performances like electrical and thermal conductivity, and tribological.
- Synergistic hybrid interaction can also construct a 3D nanofiller network which is very effective in refining the composite properties. To improve the mechanical performance of the nanocomposite, the 3D filler construction can provide a substantial area for a stress transfer platform, a neighboring-like nanofiller connection for better minimization of stress energy, and an increase in the delay of the crack propagation. In conductivity performance, the connecting filler can result in reduced conductivity resistance, thus enhancing the conductivity properties. Meanwhile, in the barrier and tribological performance, the 3D filler network can produce a denser blockade that can hinder the penetration of aggressive molecules, improving the longevity of the material.
- Due to improved filler interaction, the improvement of the properties of the nanocomposites can be achieved at lower nanofiller concentrations. On the other hand, improved filler dispersion also makes adding a higher concentration of nanofillers without arising agglomeration inside the matrix possible, increasing the ability of

the nanofillers to ameliorate the properties of the nanocomposite.

- Nanocomposites of various properties can be designed by incorporating hybrid nanofillers of different characteristics. Combining two types of nanofillers with different inherent properties can result in nanocomposites with both the characteristics; however, by varying their ratio and concentrations, these properties can be tuned according to the desired performance.

However, designing hybrid nanocomposites that fulfill all the properties desired in single hybrid reinforcement systems remains a great challenge. Therefore, further studies must still be carried out to overcome this problem and ensure the progress of the thermoset and biothermoset nanocomposites applications. Future comprehensive studies on the methods for the synthesis, processing, and exfoliating of nanofillers, as well as the methods to prepare the nanocomposites, the most common pairs of hybrid nanofillers for certain properties and applications, and also the most appropriate nanofillers contents and ratios for particular hybrids and their target properties must still be thoroughly reviewed.

**Acknowledgments:** This work was funded by the Talent and Publication Enhancement-Research Grant (TAPE-RG) sponsored by Universiti Malaysia Terengganu (Vot 55234). The authors sincerely thank the Centre for Research Management and Innovation, Universiti Pertahanan Nasional Malaysia (UPNM) for the financial support.

**Funding information:** This research was funded by Talent and Publication Enhancement-Research Grant (TAPE-RG) sponsored by Universiti Malaysia Terengganu (Vot 55234).

**Author contributions:** Conceptualization: N.A.Z. and R.M.; validation: N.A.Z. and R.M.; resources: N.A.Z. and R.M.; writing – original draft preparation: N.A.Z., R.M., and S.M.J.; writing – review and editing: N.A.Z., R.M., S.M.J., C.M.R.G., M.A., R.A.I., and M.N.F.N.; supervision: R.M.; project administration: R.M.; funding acquisition: M.N.F.N. All authors have accepted responsibility for the entire content of this manuscript and approved its submission.

**Conflict of interest:** The authors state no conflict of interest.

## References

- [1] Alejandro Rodríguez-González J, Rubio-González C, de Jesús Ku-Herrera J, Ramos-Galicia L, Velasco-Santos C. Effect of

- seawater ageing on interlaminar fracture toughness of carbon fiber/epoxy composites containing carbon nanofillers. *J Reinforced Plast Compos.* 2018 Nov 1;37(22):1346–59.
- [2] Mustapha R, Rahmat AR, Abdul Majid R, Mustapha SNH. Vegetable oil-based epoxy resins and their composites with bio-based hardener: a short review. *Polym Technol Mater.* 2019;58(12):1311–26.
- [3] Vinod A, Sanjay MR, Suchart S, Jyotishkumar P. Renewable and sustainable biobased materials: An assessment on bio-fibers, biofilms, biopolymers and biocomposites. *J Clean Prod.* 2020 Jun;258:120978.
- [4] Thyavihalli Girijappa YG, Mavinkere Rangappa S, Parameswaranpillai J, Siengchin S. Natural fibers as sustainable and renewable resource for development of eco-friendly composites: A comprehensive review. *Front Mater.* 2019 Sep 27;6:226.
- [5] Vinay SS, Sanjay MR, Siengchin S, Venkatesh CV. Effect of Al<sub>2</sub>O<sub>3</sub> nanofillers in basalt/epoxy composites: Mechanical and tribological properties. *Polym Compos.* 2021 Apr 29;42(4):1727–40.
- [6] Ganapathy T, Sathiskumar R, Sanjay MR, Senthamaraiannan P, Saravanakumar SS, Parameswaranpillai J, et al. Effect of graphene powder on banyan aerial root fibers reinforced epoxy composites. *J Nat Fibers.* 2021 Jul 3;18(7):1029–36.
- [7] Thalib NB, Mustapha SNH, Feng CK, Mustapha R. Tailoring graphene reinforced thermoset and biothermoset composites. *Rev Chem Eng.* 2020 Jul 1;36(5):623–52.
- [8] Gouda K, Bhowmik S, Das B. A review on allotropes of carbon and natural filler-reinforced thermomechanical properties of upgraded epoxy hybrid composite. *Rev Adv Mater Sci.* 2021 Apr 27;60(1):237–75.
- [9] Chieng BW, Ibrahim NA, Wan Yunus WMZ, Hussein MZ, Loo YY. Effect of graphene nanoplatelets as nanofiller in plasticized poly(lactic acid) nanocomposites. *J Therm Anal Calorim.* 2014 Dec 29;118(3):1551–9.
- [10] Song B, Liu Z, Wang L, Dong B, Pan D, Huang Y, et al. Significantly strengthening epoxy by incorporating carbon nanotubes/graphitic carbon nitride hybrid nanofillers. *Macromol Mater Eng.* 2020 Aug 1;305(8):2000231.
- [11] Yang M, Wang X, Wang R, Qi S. The fabrication and thermal conductivity of epoxy composites with 3D nanofillers of AgNWs@SiO<sub>2</sub>&GNPs. *J Mater Sci Mater Electron.* 2017 Nov 1;28(21):16141–7.
- [12] Aussawasathien D, Hrimchum K. Carboxylic-plasma-treated nanofiller hybrids in carbon fiber reinforced epoxy composites: Dispersion and synergetic effects. *Express Polym Lett.* 2021 Mar 1;15(3):262–73.
- [13] Ribeiro H, Trigueiro JPC, Silva WM, Woellner CF, Owuor PS, Cristian Chipara A, et al. Hybrid MoS<sub>2</sub>/h-BN nanofillers as synergetic heat dissipation and reinforcement additives in epoxy nanocomposites. *ACS Appl Mater Interfaces.* 2019 Jul 10;11(27):24485–92.
- [14] Viswanathan VK, Rajaram Manoharan SR, Subramanian S, Moon A. Nanotechnology in spine surgery: A current update and critical review of the literature. *World Neurosurg.* 2019 Mar;123:142–55.
- [15] Liu SZ, Feng DC, Liu ZH, Liang JY, Ren ZJ, Zhou C, et al. Development of nanotechnology in andrology. *Transl Androl Urol.* 2020 Apr;9(2):702–8.

- [16] Bayda S, Adeel M, Tuccinardi T, Cordani M, Rizzolio F. The history of nanoscience and nanotechnology: From chemical–physical applications to nanomedicine. *Molecules*. 2019 Dec 27;25(1):112.
- [17] Sim S, Wong N. Nanotechnology and its use in imaging and drug delivery (Review). *Biomed Rep*. 2021 Mar 5;14(5):42.
- [18] Olawoyin R. Nanotechnology: The future of fire safety. *Saf Sci*. 2018 Dec;110:214–21.
- [19] Hofmann T, Lowry GV, Ghoshal S, Tufenkji N, Brambilla D, Dutcher JR, et al. Technology readiness and overcoming barriers to sustainably implement nanotechnology-enabled plant agriculture. *Nat Food*. 2020 Jul 16;1(7):416–25.
- [20] Vijay Kumar V, Balaganesan G, Lee JK, Neisiany RE, Surendran S, Ramakrishna S. A review of recent advances in nanoengineered polymer composites. *Polym*. 2019 Apr 9;11(4):644.
- [21] Akgöl S, Ulucan-Karnak F, Kuru CI, Kuşat K. The usage of composite nanomaterials in biomedical engineering applications. *Biotechnol Bioeng*. 2021 Aug 8;118(8):2906–22.
- [22] Drobny JG. Additives. In: *Handbook of thermoplastic elastomers*. William Andrew Company, UK: Elsevier; 2014. p. 17–32. <https://linkinghub.elsevier.com/retrieve/pii/B978032322136800003X>.
- [23] Mustapha R, Rahmat AR, Majid RA, Noor S, Mustapha H. Mechanical and thermal properties of montmorillonite nanoclay reinforced epoxy resin with bio-based hardener. *Mater Today Proc*. 2018;5(10):21964–72. [www.sciencedirect.com/www.materialstoday.com/proceedings2214-7853](http://www.sciencedirect.com/www.materialstoday.com/proceedings2214-7853).
- [24] Yazik MHM, Sultan MTH, Mazlan N, Talib ARA, Naveen J, Shah AUM, et al. Effect of hybrid multi-walled carbon nanotube and montmorillonite nanoclay content on mechanical properties of shape memory epoxy nanocomposite. *J Mater Res Technol*. 2020;9(3):6085–100.
- [25] Nguyen TA, Nguyen QT, Bach TP. Mechanical properties and flame retardancy of epoxy resin/nanoclay/multiwalled carbon nanotube nanocomposites. *J Chem*. 2019;2019:3105205.
- [26] Chattopadhyay PK, Basuli U, Chattopadhyay S. Studies on novel dual filler based epoxidized natural rubber nanocomposite. *Polym Compos*. 2010 May;31(5):835–46.
- [27] Megahed M, Tobbala DE, El-baky MAA. The effect of incorporation of hybrid silica and cobalt ferrite nanofillers on the mechanical characteristics of glass fiber-reinforced polymeric composites. *Polym Compos*. 2021 Jan 1;42(1):271–84.
- [28] Aliakbari M, Jazani OM, Sohrabian M. Epoxy adhesives toughened with waste tire powder, nanoclay, and phenolic resin for metal-polymer lap-joint applications. *Prog Org Coat*. 2019 Nov 1;136:105291.
- [29] Garcia-Mejia G, Saavedra-Intriago G, Rigail-Cedeño A, Rivas-Ferrín A, Tapia-Bastidas CV. Effect of silica fume and rice husk silica in bio-epoxy composites. In: *Materials Today: Proceedings*. UK: Elsevier Ltd; 2020. p. 2008–12.
- [30] Fan X, Miao JT, Yuan L, Guan Q, Gu A, Liang G. Preparation and origin of thermally resistant biobased epoxy resin with low internal stress and good UV resistance based on SiO<sub>2</sub> hybridized cellulose for light emitting diode encapsulation. *Appl Surf Sci*. 2018 Jul 31;447:315–24.
- [31] Hemath M, Mavinkere Rangappa S, Kushvaha V, Dhakal HN, Siengchin S. A comprehensive review on mechanical, electromagnetic radiation shielding, and thermal conductivity of fibers/inorganic fillers reinforced hybrid polymer composites. *Polym Compos*. 2020 Oct 14;41(10):3940–65.
- [32] Dinesh S, Kumaran P, Mohanamurugan S, Vijay R, Singaravelu DL, Vinod A, et al. Influence of wood dust fillers on the mechanical, thermal, water absorption and biodegradation characteristics of jute fiber epoxy composites. *J Polym Res*. 2020 Jan 6;27(1):9.
- [33] Chen B, Li X, Jia Y, Xu L, Liang H, Li X, et al. Fabrication of ternary hybrid of carbon nanotubes/graphene oxide/MoS<sub>2</sub> and its enhancement on the tribological properties of epoxy composite coatings. *Compos Part A Appl Sci Manuf*. 2018 Dec 1;115:157–65.
- [34] Yan H, Zhang L, Li H, Fan X, Zhu M. Towards high-performance additive of Ti<sub>3</sub>C<sub>2</sub>/graphene hybrid with a novel wrapping structure in epoxy coating. *Carbon N Y*. 2020 Feb;157:217–33.
- [35] Wu Y, Jiang F, Qiang Y, Zhao W. Synthesizing a novel fluorinated reduced graphene oxide-CeO<sub>2</sub> hybrid nanofiller to achieve highly corrosion protection for waterborne epoxy coatings. *Carbon N Y*. 2021 May;176:39–51.
- [36] Upadhyay RK, Kumar A. Effect of humidity on the synergy of friction and wear properties in ternary epoxy-graphene-MoS<sub>2</sub> composites. *Carbon N Y*. 2019 May;146:717–27.
- [37] Zhan Y, Zhang J, Wan X, Long Z, He S, He Y. Epoxy composites coating with Fe<sub>3</sub>O<sub>4</sub> decorated graphene oxide: Modified bio-inspired surface chemistry, synergistic effect and improved anti-corrosion performance. *Appl Surf Sci*. 2018 Apr;436:756–67.
- [38] Zhou S, Wu Y, Zhao W, Yu J, Jiang F, Wu Y, et al. Designing reduced graphene oxide/zinc rich epoxy composite coatings for improving the anticorrosion performance of carbon steel substrate. *Mater Des*. 2019 May;169:107694.
- [39] Mat Yazik MH, Sultan MTH, Jawaid M, Abu Talib AR, Mazlan N, Md Shah AU, et al. Effect of nanofiller content on dynamic mechanical and thermal properties of multi-walled carbon nanotube and montmorillonite nanoclay filler hybrid shape memory epoxy composites. *Polym (Basel)*. 2021 Mar 1;13(5):1–21.
- [40] Zhang B, Wang J, Chen X, Su X, Zou Y, Huo S, et al. Low content Ag-coated poly(acrylonitrile) microspheres and graphene for enhanced microwave absorption performance epoxy composites. *Mater Res Express*. 2018 Apr 1;5(4):045040.
- [41] Bajpai A, Martin R, Faria H, Ibarboure E, Carlotti S. Epoxy based hybrid nanocomposites: Fracture mechanisms, tensile properties and electrical properties. *Mater Today Proc*. 2021;34:210–6.
- [42] Suherman H, Dweiri R, Mahyoedin Y, Duskiardi D. Investigation of electrical-mechanical performance of epoxy-based nanocomposites filled with hybrid electrically conductive fillers. *Mater Res Express*. 2019 Sep 25;6(11):115010.
- [43] Pokharel P, Xiao D, Erogbogbo F, Keles O, Lee DS. A hierarchical approach for creating electrically conductive network structure in polyurethane nanocomposites using a hybrid of graphene nanoplatelets, carbon black and multi-walled carbon nanotubes. *Compos B Eng*. 2019 Mar 15;161:169–82.
- [44] Jen YM, Chang HH, Lu CM, Liang SY. Temperature-dependent synergistic effect of multi-walled carbon nanotubes and graphene nanoplatelets on the tensile quasi-static and

- fatigue properties of epoxy nanocomposites. *Polym (Basel)*. 2021 Jan 1;13(1):1–25.
- [45] Shukla MK, Sharma K. Effect of functionalized graphene/CNT ratio on the synergetic enhancement of mechanical and thermal properties of epoxy hybrid composite. *Mater Res Express*. 2019 May 17;6(8):085318.
- [46] Jen YM, Huang JC, Zheng KY. Synergistic effect of multi-walled carbon nanotubes and graphene nanoplatelets on the monotonic and fatigue properties of uncracked and cracked epoxy composites. *Polym (Basel)*. 2020 Sep 1;12(9):1895.
- [47] Zhang Y, Park M, Park SJ. Implication of thermally conductive nanodiamond-interspersed graphite nanoplatelet hybrids in thermoset composites with superior thermal management capability. *Sci Rep*. 2019 Dec 1;9(1):2893.
- [48] Ribeiro H, Trigueiro JPC, Lopes MC, Pedrotti JJ, Woellner CF, Silva WM, et al. Enhanced thermal conductivity and mechanical properties of hybrid MoS<sub>2</sub>/h-BN polyurethane nanocomposites. *J Appl Polym Sci*. 2018 Aug 10;135(30):46560.
- [49] Akpan EI, Shen X, Wetzel B, Friedrich K. Design and synthesis of polymer nanocomposites. In: *Polymer Composites with Functionalized Nanoparticles*. Amsterdam: Elsevier Science; 2019. p. 47–83.
- [50] Biron M. Composites. In: *Thermosets and Composites*. UK: Elsevier Ltd; 2013. p. 299–473. <https://linkinghub.elsevier.com/retrieve/pii/B9781455731244000067>.
- [51] Caradonna A, Badini C, Padovano E, Pietroluongo M. Electrical and thermal conductivity of epoxy-carbon filler composites processed by calendaring. *Materials*. 2019;12(9):1522.
- [52] Li Y, Zhang H, Liu Y, Wang H, Huang Z, Peijs T, et al. Synergistic effects of spray-coated hybrid carbon nanoparticles for enhanced electrical and thermal surface conductivity of CFRP laminates. *Compos Part A Appl Sci Manuf*. 2018 Feb 1;105:9–18.
- [53] Sánchez-Romate XF, Jiménez-Suárez A, Campo M, Ureña A, Prolongo SG. Electrical properties and strain sensing mechanisms in hybrid graphene nanoplatelet/carbon nanotube nanocomposites. *Sensors*. 2021 Aug 2;21(16):5530.
- [54] Guo Y, Chen S, Sun L, Yang L, Zhang L, Lou J, et al. Degradable and fully recyclable dynamic thermoset elastomer for 3D-printed wearable electronics. *Adv Funct Mater*. 2021 Feb 1;31(9):2009799.
- [55] Arif MF, Kumar S, Gupta TK, Varadarajan KM. Strong linear-piezoresistive-response of carbon nanostructures reinforced hyperelastic polymer nanocomposites. *Compos Part A Appl Sci Manuf*. 2018 Oct 1;113:141–9.
- [56] Liu Y, He D, Dubrunfaut O, Zhang A, Zhang H, Pichon L, et al. GO-CNTs hybrids reinforced epoxy composites with porous structure as microwave absorbers. *Compos Sci Technol*. 2020 Nov 10;200:108450.
- [57] Zhang B, Wang J, Peng J, Sun J, Su X, Zou Y, et al. Double-shell PANS@PANI@Ag hollow microspheres and graphene dispersed in epoxy with enhanced microwave absorption. *J Mater Sci Mater Electron*. 2019 May 30;30(10):9785–97.
- [58] Zhang B, Wang J, Wang T, Su X, Yang S, Chen W, et al. High-performance microwave absorption epoxy composites filled with hollow nickel nanoparticles modified graphene *via* chemical etching method. *Compos Sci Technol*. 2019 May 26;176:54–63.
- [59] Wu Y, Zhang X, Negi A, He J, Hu G, Tian S, et al. Synergistic effects of boron nitride (BN) nanosheets and silver (Ag) nanoparticles on thermal conductivity and electrical properties of epoxy nanocomposites. *Polym (Basel)*. 2020 Feb 12;12(2):426.
- [60] Ye Y, Yang D, Zhang D, Chen H, Zhao H, Li X, et al. POSS-tetraaniline modified graphene for active corrosion protection of epoxy-based organic coating. *Chem Eng J*. 2020 Mar 1;383:123160.
- [61] Gohari Bajestani Z, Yürüm A, Yürüm Y. Decoration of graphene sheets with Pd/Al<sub>2</sub>O<sub>3</sub> hybrid particles for hydrogen storage applications. *Int J Hydrog Energy*. 2016 Jun;41(23):9810–8.
- [62] Beatrice CAG, Moreira BR, Oliveira AD, de Passador FR, Almeida Neto GR, de Leiva DR, et al. Development of polymer nanocomposites with sodium alanate for hydrogen storage. *Int J Hydrog Energy*. 2020 Feb;45(8):5337–46.
- [63] Muthu RN, Rajashabala S, Kannan R. Synthesis and characterization of microporous hybrid nanocomposite membrane as potential hydrogen storage medium towards fuel cell applications. *Ion (Kiel)*. 2019 Aug 8;25(8):3561–75.
- [64] Saikia A, Sarmah D, Kumar A, Karak N. Bio-based epoxy/polyaniline nanofiber-carbon dot nanocomposites as advanced anticorrosive materials. *J Appl Polym Sci*. 2019 Jul 15;136(27):47744.
- [65] Panda S, Behera D, Rath P, Bastia TK. Enhanced properties of UPE/ESOA partially bio-nanocomposites reinforced with chitosan functionalized graphene nanoplatelets: an innovative approach. *Bull Mater Sci*. 2018 Aug 25;41(4):102.
- [66] Chen J, Huang X, Zhu Y, Jiang P. Cellulose nanofiber supported 3D interconnected BN nanosheets for epoxy nanocomposites with ultrahigh thermal management capability. *Adv Funct Mater*. 2017 Feb 3;27(5):1604754.
- [67] Chen B, Jia Y, Zhang M, Liang H, Li X, Yang J, et al. Tribological properties of epoxy lubricating composite coatings reinforced with core-shell structure of CNF/MoS<sub>2</sub> hybrid. *Compos Part A Appl Sci Manuf*. 2019 Jul 1;122:85–95.
- [68] Ayyagari S, Al-Haik M, Rollin V. Mechanical and electrical characterization of carbon fiber/bucky paper/zinc oxide hybrid composites. *C (Basel)*. 2018 Jan 18;4(1):6.
- [69] Vo VS, Mahouche-Chergui S, Nguyen VH, Naili S, Carbonnier B. Crucial role of covalent surface functionalization of clay nanofillers on improvement of the mechanical properties of bioepoxy resin. *ACS Sustain Chem Eng*. 2019 Sep 16;7(18):15211–20.
- [70] Esmaeili A, Sbarufatti C, Jiménez-Suárez A, Hamouda AMS, Rovatti L, Ureña A. Synergistic effects of double-walled carbon nanotubes and nanoclays on mechanical, electrical and piezoresistive properties of epoxy based nanocomposites. *Compos Sci Technol*. 2020 Nov 10;200:108459.
- [71] Zhang Y, Choi JR, Park SJ. Thermal conductivity and thermophysical properties of nanodiamond-attached exfoliated hexagonal boron nitride/epoxy nanocomposites for microelectronics. *Compos Part A Appl Sci Manuf*. 2017 Oct 1;101:227–36.
- [72] Yang SY, Lin WN, Huang YL, Tien HW, Wang JY, Ma CCM, et al. Synergetic effects of graphene platelets and carbon nanotubes on the mechanical and thermal properties of epoxy composites. *Carbon N Y*. 2011 Mar;49(3):793–803.

- [73] Subhani T, Latif M, Ahmad I, Rakha SA, Ali N, Khurram AA. Mechanical performance of epoxy matrix hybrid nanocomposites containing carbon nanotubes and nanodiamonds. *Mater Des.* 2015 Dec 15;87:436–44.
- [74] Zhang Z, Li W, Wang X, Liu W, Chen K, Gan W. Low effective content of reduced graphene oxide/silver nanowire hybrids in epoxy composites with enhanced conductive properties. *J Mater Sci Mater Electron.* 2019;30:7384–92.
- [75] Kavimani V, Stalin B, Gopal PM, Ravichandran M, Karthick A, Bharani M. Application of r-GO-MMT hybrid nanofillers for improving strength and flame retardancy of epoxy/glass fibre composites. *Adv Polym Technol.* 2021;2021:6627743.
- [76] Megahed M, Megahed AA, Agwa MA. The influence of incorporation of silica and carbon nanoparticles on the mechanical properties of hybrid glass fiber reinforced epoxy. *J Ind Text.* 2019 Aug 1;49(2):181–99.
- [77] Chatterjee S, Nafezarefi F, Tai NH, Schlagenhauf L, Nüesch FA, Chu BTT. Size and synergy effects of nanofiller hybrids including graphene nanoplatelets and carbon nanotubes in mechanical properties of epoxy composites. *Carbon N Y.* 2012 Dec;50(15):5380–6.
- [78] Sánchez-Romate XF, Artigas J, Jiménez-Suárez A, Sánchez M, Güemes A, Ureña A. Critical parameters of carbon nanotube reinforced composites for structural health monitoring applications: Empirical results versus theoretical predictions. *Compos Sci Technol.* 2019 Feb 8;171:44–53.
- [79] Avilés F, May-Pat A, López-Manchado MA, Verdejo R, Bachmatiuk A, Rummeli MH. A comparative study on the mechanical, electrical and piezoresistive properties of polymer composites using carbon nanostructures of different topology. *Eur Polym J.* 2018 Feb 1;99:394–402.
- [80] An Y, Zhang X, Wang X, Chen Z, Wu X. Nano@lignocellulose intercalated montmorillonite as adsorbent for effective Mn(II) removal from aqueous solution. *Sci Rep.* 2018 Dec 18;8(1):10863.
- [81] Wei J, Atif R, Vo T, Inam F. Graphene nanoplatelets in epoxy system: Dispersion, reaggregation, and mechanical properties of nanocomposites. *J Nanomater.* 2015;2015:1–12.
- [82] Yuan Y, Chen J. Nano-welding of multi-walled carbon nanotubes on silicon and silica surface by laser irradiation. *Nanomaterials.* 2016 Feb 24;6(3):36.
- [83] Wang BY, Lee ES, Lim DS, Kang HW, Oh YJ. Roll-to-roll slot die production of 300 mm large area silver nanowire mesh films for flexible transparent electrodes. *RSC Adv.* 2017;7(13):7540–6.
- [84] Hu J, Wang W, Yu R, Guo M, He C, Xie X, et al. Solid polymer electrolyte based on ionic bond or covalent bond functionalized silica nanoparticles. *RSC Adv.* 2017;7(87):54986–94.
- [85] Chu N, Wang J, Zhang Y, Yang J, Lu J, Yin D. Nestlike hollow hierarchical MCM-22 microspheres: Synthesis and exceptional catalytic properties. *Chem Mater.* 2010 May 11;22(9):2757–63.
- [86] Zhang Y, Wang X, Cao M. Confinedly implanted NiFe<sub>2</sub>O<sub>4</sub>-rGO: Cluster tailoring and highly tunable electromagnetic properties for selective-frequency microwave absorption. *Nano Res.* 2018 Mar 1;11(3):1426–36.
- [87] Han S, Meng Q, Pan X, Liu T, Zhang S, Wang Y, et al. Synergistic effect of graphene and carbon nanotube on lap shear strength and electrical conductivity of epoxy adhesives. *J Appl Polym Sci.* 2019 Nov 10;136(42):48056.
- [88] Campo M, Redondo O, Prolongo SG. Barrier properties of thermal and electrical conductive hydrophobic multigraphitic/epoxy coatings. *J Appl Polym Sci.* 2020 Nov 10;137(42):49281.
- [89] Kumar S, Falzon BG, Hawkins SC. Ultrasensitive embedded sensor for composite joints based on a highly aligned carbon nanotube web. *Carbon N Y.* 2019 Aug 1;149:380–9.
- [90] Huang L, Wang H, Wu P, Huang W, Gao W, Fang F, et al. Wearable flexible strain sensor based on three-dimensional wavy laser-induced graphene and silicone rubber. *Sens (Switz).* 2020 Aug 1;20(15):1–14.
- [91] Yokaribas V, Wagner S, Schneider DS, Friebertshäuser P, Lemme MC, Fritzen CP. Strain gauges based on CVD graphene layers and exfoliated graphene nanoplatelets with enhanced reproducibility and scalability for large quantities. *Sens (Switz).* 2017 Dec 18;17(12):2937.
- [92] Güemes A, Morales ARP, Fernandez-Lopez A, Sanchez-Romate XXF, Sanchez M, Ureña A. Directional response of randomly dispersed carbon nanotube strain sensors. *Sens (Switz).* 2020 May 2;20(10):2980.
- [93] Anooja JB, Dijith KS, Surendran KP, Subodh G. A simple strategy for flexible electromagnetic interference shielding: Hybrid rGO@CB-reinforced polydimethylsiloxane. *J Alloy Compd.* 2019 Oct 30;807:151678.
- [94] Jaiswal R, Agarwal K, Pratap V, Soni A, Kumar S, Mukhopadhyay K, et al. Microwave-assisted preparation of magnetic ternary core-shell nanofiller (CoFe<sub>2</sub>O<sub>4</sub>/rGO/SiO<sub>2</sub>) and their epoxy nanocomposite for microwave absorption properties. *Mater Sci Eng B Solid State Mater Adv Technol.* 2020 Dec 1;262:114711.
- [95] Chen CC, Liang WF, Nien YH, Liu HK, Yang RB. Microwave absorbing properties of flake-shaped carbonyl iron/reduced graphene oxide/epoxy composites. *Mater Res Bull.* 2017 Dec 1;96:81–5.
- [96] Weng X, Li B, Zhang Y, Lv X, Gu G. Synthesis of flake shaped carbonyl iron/reduced graphene oxide/polyvinyl pyrrolidone ternary nanocomposites and their microwave absorbing properties. *J Alloy Compd.* 2017;695:508–19.
- [97] Ning M, Kuang B, Hou Z, Wang L, Li J, Zhao Y, et al. Layer by layer 2D MoS<sub>2</sub>/rGO hybrids: An optimized microwave absorber for high-efficient microwave absorption. *Appl Surf Sci.* 2019 Mar 15;470:899–907.
- [98] Bikdeli M, Seyed Dorraji MS, Hosseini SF, Hajimiri I, Rasoulifard MH, Amani-Ghadim AR. High performance microwave shielding in green nanocomposite coating based on polyurethane *via* nickel oxide, Mn<sub>x</sub>Fe<sub>3-x</sub>O<sub>4</sub> and polyaniline nanoparticles. *Mater Sci Eng B.* 2020 Dec;262:114728.
- [99] Li B, Weng X, Wu G, Zhang Y, Lv X, Gu G. Synthesis of Fe<sub>3</sub>O<sub>4</sub>/polypyrrole/polyaniline nanocomposites by *in situ* method and their electromagnetic absorbing properties. *J Saudi Chem Soc.* 2017 May 1;21(4):466–72.
- [100] Qiu X, Wang L, Zhu H, Guan Y, Zhang Q. Lightweight and efficient microwave absorbing materials based on walnut shell-derived nano-porous carbon. *Nanoscale.* 2017 Jun 14;9(22):7408–18.
- [101] Chu W, Wang Y, Du Y, Qiang R, Tian C, Han X. FeCo alloy nanoparticles supported on ordered mesoporous carbon for enhanced microwave absorption. *J Mater Sci.* 2017 Dec 1;52(23):13636–49.
- [102] Zhang N, Huang Y, Wang M. 3D ferromagnetic graphene nanocomposites with ZnO nanorods and Fe<sub>3</sub>O<sub>4</sub> nanoparticles co-decorated for efficient electromagnetic wave absorption. *Compos B Eng.* 2018 Mar 1;136:135–42.
- [103] Xu Y, Shen G, Wu H, Liu B, Fang X, Zhang D, et al. Double-layer microwave absorber based on nanocrystalline CoFe<sub>2</sub>O<sub>4</sub> and CoFe<sub>2</sub>O<sub>4</sub>/PANI multi-core/shell composites. *Mater Science-Poland.* 2017 Feb 24;35(1):94–104.



- [104] Huang Z, Chen H, Huang Y, Ge Z, Zhou Y, Yang Y, et al. Ultra-broadband wide-angle terahertz absorption properties of 3D graphene foam. *Adv Funct Mater.* 2018 Jan;28(2):1704363.
- [105] Zhao H, Cheng Y, Lv H, Ji G, Du Y. A novel hierarchically porous magnetic carbon derived from biomass for strong lightweight microwave absorption. *Carbon N Y.* 2019 Feb;142:245–53.
- [106] Zhao T, Jin W, Ji X, Yan H, Jiang Y, Dong Y, et al. Synthesis of sandwich microstructured expanded graphite/barium ferrite connected with carbon nanotube composite and its electromagnetic wave absorbing properties. *J Alloy Compd.* 2017 Jul;712:59–68.
- [107] Qing Y, Nan H, Luo F, Zhou W. Nitrogen-doped graphene and titanium carbide nanosheet synergistically reinforced epoxy composites as high-performance microwave absorbers. *RSC Adv.* 2017;7(44):27755–61.
- [108] Agarwal K, Prasad M, Katiyar M, Jaiswal R, Kumar S, Prasad NE. Study of electromagnetic properties of fabricated NiFe<sub>2</sub>O<sub>4</sub>/polyurethane nanocomposites. *J Appl Polym Sci.* 2020 Jul 15;137(27):48645.
- [109] Ribeiro H, Trigueiro JPC, Woellner CF, Pedrotti JJ, Miquita DR, Silva WM, et al. Higher thermal conductivity and mechanical enhancements in hybrid 2D polymer nanocomposites. *Polym Test.* 2020 Jul;87:106510.
- [110] Gu J, Xu S, Zhuang Q, Tang Y, Kong J. Hyperbranched polyborosilazane and boron nitride modified cyanate ester composite with low dielectric loss and desirable thermal conductivity. *IEEE Trans Dielectr Electr Insulation.* 2017 Apr;24(2):784–90.
- [111] Tian X, Li Y, Chen Z, Li Q, Hou L, Wu J, et al. Shear-assisted production of few-layer boron nitride nanosheets by supercritical CO<sub>2</sub> exfoliation and its use for thermally conductive epoxy composites. *Sci Rep.* 2017 Dec 19;7(1):17794.
- [112] Zhang X, Zhang J, Li C, Wang J, Xia L, Xu F, et al. Endowing the high efficiency thermally conductive and electrically insulating composites with excellent antistatic property through selectively multilayered distribution of diverse functional fillers. *Chem Eng J.* 2017 Nov;328:609–18.
- [113] Kim HS, Kim JH, Kim WY, Lee HS, Kim SY, Khil MS. Volume control of expanded graphite based on inductively coupled plasma and enhanced thermal conductivity of epoxy composite by formation of the filler network. *Carbon N Y.* 2017 Aug;119:40–6.
- [114] Su Z, Wang H, Ye X, Tian K, Huang W, Guo Y, et al. Non-covalent poly (2-ethylhexyl acrylate) (P2EHA)/functionalized graphene/h-boron nitride flexible composites with enhanced adhesive and thermal conductivity by a facilitated latex approach. *Compos Part A Appl Sci Manuf.* 2017 Aug;99:176–85.
- [115] Barani Z, Mohammadzadeh A, Geremew A, Huang C, Coleman D, Mangolini L, et al. Thermal properties of the binary-filler hybrid composites with graphene and copper nanoparticles. *Adv Funct Mater.* 2020 Feb 11;30(8):1904008.
- [116] Lebon A, Carrete J, Gallego LJ, Vega A. Ti-decorated zigzag graphene nanoribbons for hydrogen storage. A van der Waals-corrected density-functional study. *Int J Hydrog Energy.* 2015 Apr;40(14):4960–8.
- [117] George L, Saxena SK. Structural stability of metal hydrides, alanates and borohydrides of alkali and alkali-earth elements: A review. *Int J Hydrog Energy.* 2010 Jun;35(11):5454–70.
- [118] Oliveira AD, Beatrice CAG, Passador FR, Pessan LA. Polyetherimide-based nanocomposites materials for hydrogen storage. In *AIP Conference Proceedings*; 2016. p. 040006.
- [119] Gadipelli S, Guo ZX. Graphene-based materials: Synthesis and gas sorption, storage and separation. *Prog Mater Sci.* 2015 Apr;69:1–60.
- [120] Fang J, Levchenko I, Lu X, Mariotti D, Ostrikov KK. Hierarchical bi-dimensional alumina/palladium nanowire nano-architectures for hydrogen detection, storage and controlled release. *Int J Hydrog Energy.* 2015 May;40(18):6165–72.
- [121] Gagnon-Thibault É, Cossement D, Guillet-Nicolas R, Masoumifard N, Bénard P, Kleitz F, et al. Nanoporous ferrocene-based cross-linked polymers and their hydrogen sorption properties. *Microporous Mesoporous Mater.* 2014 Apr;188:182–9.
- [122] Schneemann A, White JL, Kang S, Jeong S, Wan LF, Cho ES, et al. Nanostructured metal hydrides for hydrogen storage. *Chem Rev.* 2018 Nov 28;118(22):10775–839.
- [123] Milanese C, Jensen TR, Hauback BC, Pistidda C, Dornheim M, Yang H, et al. Complex hydrides for energy storage. *Int J Hydrog Energy.* 2019 Mar;44(15):7860–74.
- [124] Acuña P, Zhang J, Yin GZ, Liu XQ, Wang DY. Bio-based rigid polyurethane foam from castor oil with excellent flame retardancy and high insulation capacity *via* cooperation with carbon-based materials. *J Mater Sci.* 2021 Jan 23;56(3):2684–701.
- [125] An XP, Chen JH, Li YD, Zhu J, Zeng JB. Rational design of sustainable polyurethanes from castor oil: towards simultaneous reinforcement and toughening. *Sci China Mater.* 2018 Jul 16;61(7):993–1000.
- [126] Roy K, Poompiew N, Pongwisuthiruchte A, Potiyaraj P. Application of different vegetable oils as processing aids in industrial rubber composites: A sustainable approach. *ACS Omega.* 2021 Nov 30;6(47):31384–9.
- [127] Jia P, Xia H, Tang K, Zhou Y. Plasticizers derived from biomass resources: A short review. *Polym (Basel).* 2018 Nov 24;10(12):1303.
- [128] Sanay B, Strehmel B, Strehmel V. Formation of highly crosslinked polymer films in the presence of bio-based epoxy by photoinitiated cationic polymerization. *Prog Org Coat.* 2021 Sep;158:106377.
- [129] Ilyas RA, Zuhri MYM, Aisyah HA, Asyraf MRM, Hassan SA, Zainudin ES, et al. Natural fiber-reinforced polylactic acid, polylactic acid blends and their composites for advanced applications. *Polym (Basel).* 2022;14(1):202.
- [130] Ilyas RA, Aisyah HA, Nordin AH, Ngadi N, Zuhri MYM, Asyraf MRM, et al. Natural-fiber-reinforced chitosan, chitosan blends and their nanocomposites for various advanced applications. *Polym (Basel).* 2022;14(5):874.
- [131] Ilyas RA, Zuhri MYM, Norrrahim MNF, Misenan MSM, Jenol MA, Samsudin SA, et al. Natural fiber-reinforced polycaprolactone green and hybrid biocomposites for various advanced applications. *Polym (Basel).* 2022;14(1):182.
- [132] Norfarhana AS, Ilyas RA, Ngadi N. A review of nanocellulose adsorptive membrane as multifunctional wastewater treatment. *Carbohydr Polym.* 2022;291:119563.
- [133] Ilyas, RA, Sapuan, SM, Harussani, MM, Hakimi, MYAY, Haziq, MZM, Atikah, MSN, et al. Polylactic acid (PLA) biocomposite: Processing, additive manufacturing and advanced applications. *Polym (Basel).* 2021;13(8):1326.